□ REVIEW ARTICLE □

Clinical Significance of Anti-CCP Antibodies in Rheumatoid Arthritis

Tsuneyo MIMORI

Abstract

A number of novel autoantibodies have been recently described in rheumatoid arthritis (RA), and their clinical significance and possible pathogenic roles have been discussed. In particular, new autoantibodies to citrullinated proteins such as filaggrin and its circular form (cyclic citrullinated peptide: CCP) are especially noteworthy because of their high sensitivity and high specificity. There are many studies that anti-CCP antibodies may serve as a powerful serologic marker for early diagnosis of RA and prognostic prediction of joint destruction. Anti-citrullinated protein antibodies are locally produced in RA joints, and citrullinated proteins (most are fibrins) are localized in RA synovial tissue. This finding strongly suggests a possibility that local citrullination of intraarticular proteins might be the initial event leading to autoantibody production in RA. Genetic factors such as a gene polymorphism of the citrullinating enzyme, PADI, might be associated with the breakage of self-tolerance and induction of autoimmunity against citrullinated proteins.
(Internal Medicine 44: 1122–1126, 2005)

Key words: citrullinated protein, filaggrin, peptidylarginine deiminase, autoantibody

Introduction

Rheumatoid arthritis (RA) is a systemic inflammatory disease characterized by chronic and erosive polyarthritis by abnormal growth of synovial tissue or pannus, and causes irreversible joint disability. Recent studies show that joint injury in RA patients progresses within 2 years from onset, and aggressive treatments from the early stage can prevent the following progression of the disease. Hence, the necessities of early diagnosis and early treatment have been emphasized. However, RA patients do not always show typical symptoms and signs at their early stage, and are often difficult to be diagnosed since they may not fulfill the classification criteria for RA.

RA is also categorized among systemic autoimmune diseases because of the presence of rheumatoid factor (RF), autoantibodies against the Fc portion of IgG, and other autoantibodies. RF has been clinically utilized as the only serologic marker of RA so far. However, the sensitivity of RF is 60–80% in RA, and the specificity is rather low since RF is also detected widely and frequently in many other conditions including various connective tissue diseases, chronic liver diseases and infectious diseases, and even in a few healthy people. Therefore, despite the fact that RF is adopted into the criteria for classification of RA, its diagnostic value is unsatisfactory especially in the early disease.

In recent years, a number of novel autoantibodies have been described in RA, and their clinical significance and possible pathogenic roles have been discussed. In particular, new autoantibodies to citrullinated proteins such as filaggrin and its circular form (cyclic citrullinated peptide: CCP) are the most remarkable because of the reasonable sensitivity and high specificity in RA patients, which may be able to serve as an early diagnostic marker and a prognostic factor of joint destruction. This article reviews and discusses the nature of target autoantigens as well as clinical and possible etiopathogenic significance of anti-citrullinated antibodies in RA.

Identification of Citrullinated Proteins as RA-specific Autoantigens

In the 1960s, autoantibodies termed as anti-perinuclear factor (APF) were first described as RA-specific autoantibodies, which react with keratohyaline granules scattered around the perinuclear region of human buccal epithelial cells in indirect immunofluorescence (1). In the 1970s, so-called anti-"keratin" antibodies (AKA) were reported as other RA-specific autoantibodies recognized by indirect

From Department of Rheumatology and Clinical Immunology, Kyoto University Graduate School of Medicine, Kyoto
Reprint requests should be addressed to Dr. Tsuneyo Mimori, Department of Rheumatology and Clinical Immunology, Kyoto University Graduate School of Medicine, 54 Shogoin-Kawahara-cho, Sakyo-ku, Kyoto 606-8507

immunofluorescent study using rat esophagus cryostat section (2). Although termed as AKA since the keratin-like structure in the cornified layer of esophageal epithelia was specifically stained, the true target antigen had not been clarified. These two antibodies appeared to be highly specific for RA patients, and had been suspected as the same autoantibodies since they tended to be detected simultaneously. However, these autoantibodies had not been in routine clinical use, since target antigens were not identified and there were some practical difficulties in detecting techniques.

In 1993, Simon et al found that 75% of RA patient sera recognized a 40 kDa protein isolated from human skin tissue (3). They finally demonstrated that this protein was the target antigen of AKA by absorption study, and was a molecule called filaggrin by peptide mapping, which was involved in the aggregation of intracellular cytokeratin filaments. They further recognized that AKA and APF had almost the same specificity, because the target molecule of APF was profilaggrin, the precursor molecule of filaggrin (4).

Filaggrin is produced at first as profilaggrin of ~400 kDa in the late stage of skin differentiation and stored in keratohyaline granules of keratinocytes. Profilaggrin is a phosphorylated protein with 10–12 repeated motifs of 324 amino acid sequences (filaggrin unit), which is dephosphorylated and cleaved during keratinization, and turns to filaggrin molecules. Furthermore, arginine residues of filaggrin molecules are converted to citrullines by an enzyme peptidylarginine deiminase (PADI). These citrulline residues on the filaggrin are important for epitopes recognized by RA autoantibodies (5).

Cyclic citrullinated peptide (CCP) is an artificial molecule in which two serine residues in a major epitope peptide from filaggrin are converted to cysteine and the circular form is made by S-S bond (first generation of CCP). It has been reported that the sensitivity in RA patients was increased and the specificity was unchanged by using CCP as the antigen for ELISA (6). However, the results of anti-filaggrin and anti-CCP antibodies are not always identical, suggesting the diversity of autoantigenic epitopes of citrullinated peptides recognized by the heterogeneous population of autoantibodies (5).

Anti-Sa antibodies were reported as RA-specific autoantibodies that recognized an unknown 50 kDa doublet protein in human spleen and placenta extracts. Anti-Sa antibodies are detected in 31–43% of RA patients with very high specificity (>98%) by immunoblotting (7–9). The target Sa antigen was later identified as a citrullinated vimentin (10). Therefore, anti-Sa antibodies are one of the family members of autoantibodies reactive with citrullinated proteins as well as APF, AKA, anti-filaggrin and anti-CCP antibodies.

It is suspected that the filaggrin molecule distributed in the skin and other keratinated epithelia becomes the target of autoimmune response in the joint-affected disease. However, as discussed later, a possibility has been postulated that citrullination of proteins in the joint, rather than the filaggrin molecule itself, may be involved in the autoantibody production and the etiopathogenesis of RA.

Clinical Significance of Anti-citrullinated Protein Antibodies in Diagnosis of RA

To date, a number of reports have demonstrated the clinical significance of autoantibodies to citrullinated filaggrin and CCP in the diagnosis of RA as summarized in Table 1 (3, 5, 6, 11–14). Although the specificity of anti-filaggrin/CCP antibodies in RA is more than 90% in almost all reports, the prevalence (sensitivity) of the same antibodies ranges from 33% to 87.2%. Such a discrepancy in sensitivity might reflect racial and genetic backgrounds as well as the differences of used antigens and detection techniques among reports. In earlier studies, natural filaggrins have been used, and then citrullinated recombinant filaggrins and CCP have been utilized. Generally, anti-CCP appears to be more sensitive than anti-filaggrin. Furthermore, the second generation kit of anti-CCP test has been recently developed, in which highly reactive peptides are selected from random peptide library and are used as antigens for ELISA. The second generation kits maintain the high specificity and have the more improved sensitivity than the first generation kits. Many recent reports of anti-CCP antibodies from Japan have used the second generation kits, and the most of them describe that the sensitivity of anti-CCP in RA is as high as that of RF or even higher.

Anti-citrullinated protein antibodies can be detected in RA patient sera from early stage of the disease. Schellekens et al described that anti-CCP antibodies were detected in 68% of RA patients. Although the sensitivity was decreased to 48% in early RA cases, still the high specificity was maintained at 96% (6). In particular, the combination of anti-CCP and IgM-RF revealed a high positive predictive value for RA. In the report of van Gaalen et al, from 318 patients with undifferentiated arthritis at the first visit, RA had later developed in 93% with positive anti-CCP and in only 25% with negative anti-CCP antibodies (OR=37.8) (15). Rantapää-Dahlqvist et al reported that when preserved sera from 83 cases who had been registrated as blood donors and later developed RA were studied, anti-CCP antibodies were detected in 33.7% from the disease-free period (16). A similar result was described in the study of serial measurement in blood donors by Nielen et al, in which 49% of RA patients were positive for IgM-RF and/or anti-CCP before the development of RA symptoms (median of 4.5 years before onset, range 0.1–13.8 years) (17).

Anti-citrullinated protein antibodies may be useful as a new serologic marker for RA, because of their high specificity and high sensitivity in RA, and may also serve as an early diagnostic marker.

Correlation Between Anti-citrullinated Protein Antibodies and Disease Severity

There have been several reports that anti-citrullinated

Table 1. Clinical Significance of Anti-filaggrin/CCP Antibodies in RA

Author (year)	Subjects	Antigens (Methods)*	Sensitivity	Specificity	Ref. No.
Simon (1993)	RA 48/control 56	human skin FA (IB)	75%	89%	3
Schellekens (1998)	RA 134/control 154	CCP (ELISA)	76%	96%	5
Schellekens (2000)	RA 134/control 154	CCP (ELISA)	68%	98%	6
	early arthritis 486	CCP (ELISA)	48%	96%	
Goldbach-Mansky	arthritis <1 year 238	human skin FA (ELISA)	33%	93%	11
(2000)	(RA 106/others 122)	CCP (ELISA)	41%	91%	
Bizzaro (2001)	RA 98/control 232	CCP (ELISA)	41%	97.8%	12
Vincent (2002)	RA 240/control 471	rat r-cFA (ELISA)	67%	98.5%	13
		human r-cFA (IB)	48%		
		CCP (ELISA)	58%		
Suzuki (2003)	RA 549/control 208	CCP (ELISA)	87.6%	88.9%	14
		human r-cFA (ELISA)	68.7%	94.7%	
Rantapää-Dahlqvist (2003)	RA 83 from blood donors before onset	CCP (ELISA)	33.7%	98.2%	16

*FA: filaggrin, r-cFA: recombinant citrullinated filaggrin, IB: immunoblotting, ELISA: enzyme-linked immunosorbant assay.

Table 2. Reports of Anti-citrullinated Antibodies as a Predictive Factor for Prognosis of RA

Author (year)	Subjects	Antibodies (Methods)*	Predictability	Other prognostic factors	Ref. No.
Schellekens (2000)	RA 144	αCCP (ELISA)	+	IgM-RF	6
Kroot (2000)	early RA 273	αCCP (ELISA)	+	baseline X-ray, RF	18
Bas (2000)	RA 119	AFA (ELISA)	–	RF	23
Forslind (2001)	early RA 112	AFA (IB)	+		19
		AKA (IF)	+		
Paimela (2001)	early RA 78	AFA (ELISA)	–		24
Meyer (2003)	early RA 191	αCCP (ELISA)	+		21
		APF (IF)	+		
		AKA (IF)	–		
Rantapää-Dahlqvist (2003)	RA 83 (blood donors)	αCCP (ELISA)	+	IgA-RF	16
Forslind (2004)	early RA 378	αCCP (ELISA)	+	baseline Larsen score, ESR	20

*AFA: anti-filaggrin antibodies, AKA: anti-keratin antibodies, APF: anti-perinuclear factor, ELISA: enzyme-linked immunosorbant assay, IB: immunoblotting, IF: immunofluorescence.

protein antibodies might be a predictive marker for the progression of joint destruction as summarized in Table 2. Schellekens et al described that both anti-CCP and IgM-RF at the first visit predicted erosive change at 2 years follow-up in RA patients with 91% of positive predictive value (6). Kroot et al reported that anti-CCP was positive in 70% of 273 RA patients who had had disease symptoms for less than 1 year at study entry, and patients with anti-CCP had developed significantly more severe radiological damage after 6 years follow-up (18). In multiple regression analysis, radiological damage after 6 years follow-up was significantly predicted by IgM-RF, radiological score at entry and anti-CCP status. Forslind et al measured anti-filaggrin antibodies by immunoblotting and AKA in 112 patients with early RA, and showed that positive anti-filaggrin or AKA patients at baseline had significantly higher Larsen scores in 5 years later than the patients without these antibodies (19). Later, they also reported the role of anti-CCP in the radiological outcome in 379 cases with early RA, and concluded that anti-CCP as well as the baseline Larsen score and ESR was an independent predictor of radiological damage and progression in multiple regression analysis (20). In the reports of Meyer et al, in which 191 RA patients within one-year onset were followed up, the likelihood of a total Sharp score increase after 5 years was significantly higher among patients with anti-CCP or APF but not RF and AKA (21). Visser et al showed that anti-CCP had a high discriminating power between persistent and self-limiting arthritis and between erosive and non-erosive arthritis in his clinical prediction model of arthritis outcome (22).

While these reports showed anti-CCP as a good prognostic marker of radiological progression in RA patients, there

are also several reports that anti-filaggrin antibodies are not associated with the disease severity. Bas et al measured anti-filaggrin in 199 RA patients and the severity of erosion for a given disease duration was correlated only with RF but not with anti-filaggrin (23). In the report of Paimela et al in which the human skin filaggrin was used as an antigen for ELISA, raised anti-filaggrin levels at entry were associated with an active and treatment-resistant disease, but did not predict radiological progression (24).

As reviewed here, all reports of anti-CCP indicate a positive correlation with radiological progression, whereas anti-filaggrin and AKA tend to be independent of the disease severity (Table 2). This discrepancy may reflect heterogeneity of autoantigenic epitopes on citrullinated filaggrin molecules, and suggest a possibility that clinical significance may vary among different epitopes and different techniques.

Protein Citrullination and Etiopathogenesis of RA

Citrullinated proteins are observed in the synovial tissue of RA joints but not in normal joints. Citrulline is expressed mainly in the lining and sublining layers intracellularly or found in interstitial amorphous deposits of RA synovium (25, 26). These citrullinated proteins are not filaggrin but were identified as citrullinated forms of the α- and β-chains of fibrin (26). Recently, the target antigen of anti-Sa antibodies that were reported as RA-specific autoantibodies was identified as citrullinated vimentin. Thus, various citrullinated proteins and peptides have been demonstrated as the specific autoantigens in RA. These results strongly suggest a possibility that citrullinated proteins deposited in the RA synovium are the major targets of autoimmune response in RA patients. In addition, B cells from the synovial fluid, but not peripheral blood B cells, of anti-CCP-positive RA patients spontaneously produce anti-CCP antibodies (27). This fact suggests that an antigen-driven activation of B cells specific for citrullinated proteins occurs at the site of inflammation in RA.

Recently, an interesting report concerning the correlation between the gene polymorphism of the citrullinating enzyme, PADI, and RA susceptibility has been published (28). Japanese researchers conducted a genome-wide screening by SNPs analysis to identify the disease-susceptibility genes for Japanese patients with RA. In this study, the PADI type 4 (PADI4) gene, one of the genes of four types of PADI that are located in chromosome 1p36, was identified as the locus of RA-susceptibility gene. One of the haplotypes (haplotype 2) of PADI4 was found more frequently in RA patients (32%) than in normal controls (25%) (OR=1.97) and was thought to be the RA-susceptible haplotype. The PADI4 was mainly expressed in bone marrow cells and peripheral leukocytes and monocytes as well as RA synovium. Moreover, it was demonstrated that mRNA expressed from the RA-susceptible form of PADI4 had a longer half life than mRNA from the RA-non-susceptible PADI4, and RA patients who had the homozygous RA-susceptible haplotype developed more frequent anti-filaggrin antibodies. These data suggest a possibility that proteins might be easily citrullinated in RA patients, and over-citrullinated proteins such as citrullinated fibrin in the joints might break self-tolerance and promote abnormal immune response.

However, there is also another report against this hypothesis. Shortly after the above study published, Barton et al reported that no correlation was found between RA patients in UK and the PADI4 polymorphism (29). Although the genetic and racial background may be the cause of this discrepancy, further studies will be needed to clarify the role of protein citrullination on the etiopathogenesis of RA.

Conclusion

In recent studies, it has been demonstrated that RA patients produce not only RF but also a variety of other autoantibodies. Although most of the autoantibodies are not always specific for RA, autoantibodies to citrullinated proteins (APF, AKA, anti-filaggrin, anti-CCP and anti-Sa) appear to be exclusively detected in RA. Anti-CCP antibodies are especially noteworthy because of their high sensitivity as well as high specificity. These antibodies may serve as a powerful serologic marker for early diagnosis and prognostic prediction of RA. New criteria for the early diagnosis or classification of RA should be considered if the routine test of these RA-specific autoantibodies could be utilized. Anti-citrullinated protein antibodies are locally produced in RA joints, and citrullinated proteins identified as citrullinated fibrins are localized in RA synovial tissue. These findings strongly suggest a possibility that local citrullination of intraarticular proteins might be the initial event leading to autoantibody production in RA. Genetic factors such as HLA and a gene polymorphism of the citrullinating enzyme, PADI, (that might express more stable mRNA and cause over-citrullination of proteins) might be associated with the breakage of self-tolerance and induction of autoimmunity against citrullinated proteins. Further research however will be necessary to elucidate the fine mechanism and significance of protein citrullination in etiopathogenesis of RA.

References

1) Nienhuis RLF, Mandema E. A new serum factor in patients with rheumatoid arthritis: the antiperinuclear factor. Ann Rheum Dis **23**: 302–305, 1964.
2) Young BJ, Mallya RK, Leslie RD, Clark CJ, Hamblin TJ. Anti-keratin antibodies in rheumatoid arthritis. Br Med J **2**: 97–99, 1979.
3) Simon M, Girbal E, Sebbag M, et al. The cytokeratin filament-aggregating protein filaggrin is the target of the so-called "antikeratin antibodies," autoantibodies specific for rheumatoid arthritis. J Clin Invest **92**: 1387–1393, 1993.
4) Sebbag M, Simon M, Vincent C, et al. The antiperinuclear factor and the so-called antikeratin antibodies are the same rheumatoid arthritis-specific autoantibodies. J Clin Invest **95**: 2672–2679, 1995.
5) Schellekens GA, de Jong BA, van den Hoogen FH, van de Putte LB, van Venrooij WJ. Citrulline is an essential constituent of antigenic

determinants recognized by rheumatoid arthritis-specific autoantibodies. J Clin Invest **101**: 273–281, 1998.
6) Schellekens GA, Visser H, de Jong BA, et al. The diagnostic properties of rheumatoid arthritis antibodies recognizing a cyclic citrullinated peptide. Arthritis Rheum **43**: 155–163, 2000.
7) Despres N, Boire G, Lopez-Longo FJ, Menard HA. The Sa system: a novel antigen-antibody system specific for rheumatoid arthritis. J Rheumatol **21**: 1027–1033, 1994.
8) Hueber W, Hassfeld W, Smolen JS, Steiner G. Sensitivity and specificity of anti-Sa autoantibodies for rheumatoid arthritis. Rheumatology (Oxford) **38**: 155–159, 1999.
9) Hayem G, Chazerain P, Combe B, et al. Anti-Sa antibody is an accurate diagnostic and prognostic marker in adult rheumatoid arthritis. J Rheumatol **26**: 7–13, 1999 (Erratum in: J Rheumatol **26**: 2069, 1999).
10) Vossenaar ER, Despres N, Lapointe E, et al. Rheumatoid arthritis specific anti-Sa antibodies target citrullinated vimentin. Arthritis Res Ther **6**: R142–150, 2004.
11) Goldbach-Mansky R, Lee J, McCoy A, et al. Rheumatoid arthritis associated autoantibodies in patients with synovitis of recent onset. Arthritis Res **2**: 236–243, 2000.
12) Bizzaro N, Mazzanti G, Tonutti E, Villalta D, Tozzoli R. Diagnostic accuracy of the anti-citrulline antibody assay for rheumatoid arthritis. Clin Chem **47**: 1089–1093, 2001.
13) Vincent C, Nogueira L, Sebbag M, et al. Detection of antibodies to deiminated recombinant rat filaggrin by enzyme-linked immunosorbent assay: a highly effective test for the diagnosis of rheumatoid arthritis. Arthritis Rheum **46**: 2051–2058, 2002.
14) Suzuki K, Sawada T, Murakami A, et al. High diagnostic performance of ELISA detection of antibodies to citrullinated antigens in rheumatoid arthritis. Scand J Rheumatol **32**: 197–204, 2003.
15) van Gaalen FA, Linn-Rasker SP, van Venrooij WJ, et al. Autoantibodies to cyclic citrullinated peptides predict progression to rheumatoid arthritis in patients with undifferentiated arthritis: a prospective cohort study. Arthritis Rheum **50**: 709–715, 2004.
16) Rantapää-Dahlqvist S, de Jong BA, Berglin E, et al. Antibodies against cyclic citrullinated peptide and IgA rheumatoid factor predict the development of rheumatoid arthritis. Arthritis Rheum **48**: 2741–2749, 2003.
17) Nielen MM, van Schaardenburg D, Reesink HW, et al. Specific autoantibodies precede the symptoms of rheumatoid arthritis: a study of serial measurements in blood donors. Arthritis Rheum **50**: 380–386, 2004.
18) Kroot EJ, de Jong BA, van Leeuwen MA, et al. The prognostic value of anti-cyclic citrullinated peptide antibody in patients with recent-onset rheumatoid arthritis. Arthritis Rheum **43**: 1831–1835, 2000.
19) Forslind K, Vincent C, Serre G, Svensson B. Antifilaggrin antibodies in early rheumatoid arthritis may predict radiological progression. Scand J Rheumatol **30**: 221–224, 2001.
20) Forslind K, Ahlmen M, Eberhardt K, Hafstrom I, Svensson B; BARFOT Study Group. Prediction of radiological outcome in early rheumatoid arthritis in clinical practice: role of antibodies to citrullinated peptides (anti-CCP). Ann Rheum Dis **63**: 1090–1095, 2004.
21) Meyer O, Labarre C, Dougados M, et al. Anticitrullinated protein/peptide antibody assays in early rheumatoid arthritis for predicting five year radiographic damage. Ann Rheum Dis **62**: 120–126, 2003.
22) Visser H, le Cessie S, Vos K, Breedveld FC, Hazes JM. How to diagnose rheumatoid arthritis early: a prediction model for persistent (erosive) arthritis. Arthritis Rheum **46**: 357–365, 2002.
23) Bas S, Perneger TV, Mikhnevitch E, et al. Association of rheumatoid factors and anti-filaggrin antibodies with severity of erosions in rheumatoid arthritis. Rheumatology (Oxford) **39**: 1082–1088, 2000.
24) Paimela L, Palosuo T, Aho K, et al. Association of autoantibodies to filaggrin with an active disease in early rheumatoid arthritis. Ann Rheum Dis **60**: 32–35, 2001.
25) Baeten D, Peene I, Union A, et al. Specific presence of intracellular citrullinated proteins in rheumatoid arthritis synovium: relevance to antifilaggrin autoantibodies. Arthritis Rheum **44**: 2255–2262, 2001.
26) Masson-Bessiere C, Sebbag M, Girbal-Neuhauser E, et al. The major synovial targets of the rheumatoid arthritis-specific antifilaggrin autoantibodies are deiminated forms of the alpha- and beta-chains of fibrin. J Immunol **166**: 4177–4184, 2001.
27) Reparon-Schuijt CC, van Esch WJ, van Kooten C, et al. Secretion of anti-citrulline-containing peptide antibody by B lymphocytes in rheumatoid arthritis. Arthritis Rheum **44**: 41–47, 2001.
28) Suzuki A, Yamada R, Chang X, et al. Functional haplotypes of PADI4, encoding citrullinating enzyme peptidylarginine deiminase 4, are associated with rheumatoid arthritis. Nat Genet **34**: 395–402, 2003.
29) Barton A, Bowes J, Eyre S, et al. A functional haplotype of the PADI4 gene associated with rheumatoid arthritis in a Japanese population is not associated in a United Kingdom population. Arthritis Rheum **50**: 1117–1121, 2004.

Role of membrane sphingomyelin and ceramide in platform formation for Fas-mediated apoptosis

Michihiko Miyaji,[1,2] Zhe-Xiong Jin,[1,3] Shohei Yamaoka,[4] Ryuichi Amakawa,[2] Shirou Fukuhara,[2] Satoshi B. Sato,[5,6] Toshihide Kobayashi,[5] Naochika Domae,[7] Tsuneyo Mimori,[1] Eda T. Bloom,[8] Toshiro Okazaki,[4] and Hisanori Umehara[1,3]

[1]Department of Rheumatology and Clinical Immunology, Graduate School of Medicine, Kyoto University, Sakyo-ku, Kyoto 606-8507, Japan
[2]First Department of Internal Medicine, Kansai Medical University, Moriguchi, Osaka 570-8506, Japan
[3]Division of Hematology and Immunology, Department of Internal Medicine, Kanazawa Medical University, Ishikawa 920-0293, Japan
[4]Department of Clinical Laboratory Medicine/Hematology, Faculty of Medicine, Tottori University, Yonago, Tottori 683-8504, Japan
[5]RIKEN, Wako, Saitama 351-0198, Japan
[6]Department of Biophysics, Graduate School of Science, Kyoto University, Kyoto 606-8502, Japan
[7]Department of Medicine, Osaka Dental University, Hirakata, Osaka 573-1121, Japan
[8]Division of Cellular and Gene Therapies, Center for Biologics Evaluation and Research, Food and Drug Administration, Bethesda, MD 20892

Engagement of the Fas receptor (CD95) initiates multiple signaling pathways that lead to apoptosis, such as the formation of death-inducing signaling complex (DISC), activation of caspase cascades, and the generation of the lipid messenger, ceramide. Sphingomyelin (SM) is a major component of lipid rafts, which are specialized structures that enhance the efficiency of membrane receptor signaling and are a main source of ceramide. However, the functions of SM in Fas-mediated apoptosis have yet to be clearly defined, as the responsible genes have not been identified. After cloning a gene responsible for SM synthesis, *SMS1*, we established SM synthase–defective WR19L cells transfected with the human Fas gene (WR/Fas-SM(−)), and cells that have been functionally restored by transfection with *SMS1* (WR/Fas-SMS1). We show that expression of membrane SM enhances Fas-mediated apoptosis through increasing DISC formation, activation of caspases, efficient translocation of Fas into lipid rafts, and subsequent Fas clustering. Furthermore, WR/Fas-SMS1 cells, but not WR/Fas-SM(−) cells, showed a considerable increase in ceramide generation within lipid rafts upon Fas stimulation. These data suggest that a membrane SM is important for Fas clustering through aggregation of lipid rafts, leading to Fas-mediated apoptosis.

CORRESPONDENCE
Hisanori Umehara:
umehara@kanazawa-med.ac.jp

Abbreviations used: aSMase; acid sphingomyelinase, CTx; choleratoxin B; $\Delta\Psi$m, mitochondrial membrane potential; DISC, death-inducing signaling complex; FADD, Fas-associated death domain; FasL, Fas ligand; MBP, maltose-binding protein; PI, propidium iodide; SM; sphingomyelin.

Fas, also known as CD95, is a death domain–containing member of the TNFR super family (1). Currently, two distinct pathways that require different initiator caspases (caspase-8, -9, and -10) but converge at activation of executor caspases (caspase-3, -6, and -7) are proposed in Fas-mediated apoptosis signaling (2, 3). In type I cell apoptosis (mitochondrion independent), engagement by Fas ligand (FasL), or anti-Fas antibody (CH11), leads to receptor trimerization and recruitment of the cytoplasmic adaptor protein, Fas-associated death domain (FADD), and procaspase-8 and -10, thus forming a death-inducing signaling complex (DISC). On the other hand, in type II cell apoptosis (mitochondrion dependent), minimal caspase-8 can cleave the Bcl-2 family member Bid. The truncated Bid translocates to mitochondria, where it perturbs the mitochondrial membrane potential ($\Delta\Psi$m) and facilitates the formation of mitochondrial permeability transition pores, resulting in the release of cytochrome *c* (4).

Aggregation and clustering of cell surface receptors on binding to their specific ligands has been reported for a variety of receptors, including the TCR–CD3 complex, B cell receptor, TNFR, epithelial-derived growth factor receptor, CD2, CD44, CD11a/CD18, and Fas,

The online version of this article contains supplemental material.

and is facilitated by localization of receptor and proximal signaling components within cholesterol, glycosphingolipids, and sphingomyelin (SM)-rich membrane microdomains, known as lipid rafts (5–9). Recently, there is accumulating evidence that rafts are involved in Fas-induced apoptosis through the translocation and clustering of Fas into rafts on stimulation (7, 10, 11). Studies have reported that Fas ligation triggers translocation of the acid sphingomyelinase (aSMase) from an intracellular compartment onto the cell surface, where it hydrolyzes SM to ceramide, and that accumulation of ceramide contributes to transforming small rafts into larger signaling platforms that trap and cluster Fas (7, 10). Rafts have been detected using choleratoxin B (CTx), which binds to ganglioside GM1 colocalized in rafts, and the role of rafts has been evaluated by the disruption of rafts using the cholesterol-chelating reagent methyl-β-cyclodextrin. However, there has been no direct evidence that membrane SM, a major raft component, is involved in raft functions or Fas-mediated apoptosis. Very recently, we and others have succeeded in cloning the human cDNA for SM synthase (*SMS1*; references 12 and 13). Using SM synthesis–deficient cells, and cells in which function has been restored by transfection with the novel *SMS1* gene, we demonstrated that expression of membrane SM enhanced Fas-mediated apoptosis through efficient clustering of Fas itself with a concomitant increase in DISC formation, the activation of caspases, and the loss of $\Delta\Psi$m.

RESULTS

Characterization of SM-deficient and functionally restored cells by transfection with the SM synthase gene

Lysenin is an SM-directed cytolysin purified from the earthworm (14), which binds to membrane SM and induces pore formation in the plasma membrane and subsequent cell death (14). During investigation of the sphingolipid metabolism in SM synthase–defective WR19L mouse lymphoid cells transfected with the human *Fas* gene (WR19L/Fas; reference 15), we established membrane sphigomyelin-deficient cells, WR/Fas-SM(−), which were resistant to lysenin-mediated cell lysis. Recently, we established a functional revertant cell line, designated WR/Fas-SMS1 cells, by transfection of *SMS1* (12). WR/Fas-SMS1 cells exhibited restored SM synthesis assayed by radiolabeling of cellular lipids with [^{14}C]serine (Fig. 1 A) and recovered sensitivity against lysenin-mediated cytolysis (not depicted; reference 12).

Recently, Yamaji-Hasegawa et al. produced a mutant lysenin, which specifically binds to SM without induction of cell death (16). Using the mutant lysenin conjugated with maltose-binding protein (MBP), we examined SM expression on the plasma membrane of WR/Fas-SM(−) and WR/Fas-SMS1 cells by confocal microscopy. Expression of SM detected by lysenin–MBP plus FITC-labeled anti-MBP antibody was positive in WR/Fas-SMS1 but not in WR/Fas-SM(−) cells (Fig. 1 B). Membrane expression of ganglioside GM1 detected by FITC-labeled CTx was observed on both cells (not depicted; reference 12).

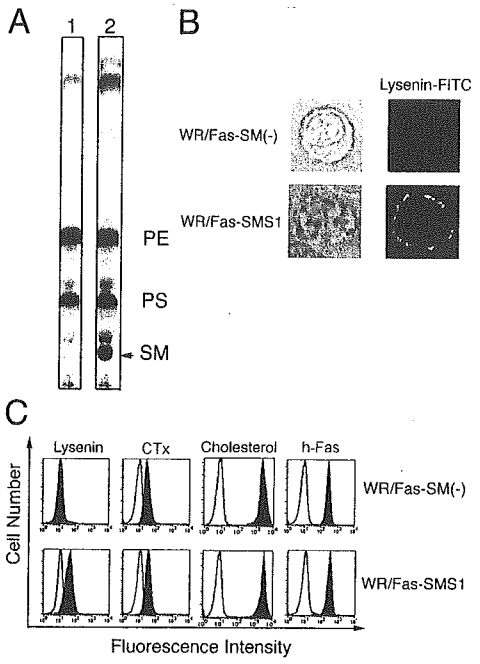

Figure 1. Characterization of WR/Fas-SM(−) and WR/Fas-SMS1 cells. (A) SM synthase activity of WR/Fas-SM(−) (lane 1) and WR/Fas-SMS1 (lane 2) cells. The cellular lipids were labeled with [^{14}C]serine, extracted by the Bligh and Dyer method (reference 53), and assessed by TLC. PE, phosphatidylethanolamine; PS, phosphatidylserine. (B) Analysis of membrane SM expression by confocal microscopy. Cells were stained with lysenin-MBP, and FITC-conjugated anti-mouse IgG mAb, then examined by laser scan confocal microscopy. (C) FACS analysis of membrane sphingolipids. To detect membrane SM, cells were stained with lysenin-MBP (Lysenin), CH11, and FITC-conjugated anti-mouse IgG mAb. Surface expression of ganglioside GM1, cholesterol, and human Fas were analyzed using FITC-conjugated CTx, cholesterol-PEG (cholesterol), or anti-Fas mAB (h-Fas), respectively.

We confirmed the accumulation of SM on the surface of WR/Fas-SM(−) and WR/Fas-SMS1 cells by FACS analysis. Binding of lysenin–MBP was positive in WR/Fas-SMS1 cells but not in WR/Fas-SM(−) cells. We also examined the expression of other lipid components of the plasma membrane, such as ganglioside GM1 and cholesterol, as well as the expression of human Fas. Binding of CTx, which binds the oligosaccharide portion of ganglioside GM1, considered to be a maker of lipid rafts, and binding of fluorescein ester of polyethylene glycol-derivatized cholesterol (fPEG-cholesterol; reference 17), which specifically binds membrane cholesterol, as well as expression of Fas, was detected equally on both cells (Fig. 1 C).

Fas-mediated apoptosis and loss of $\Delta\Psi$m in WR/Fas-SM(−) and WR/Fas-SMS1 cells

Although Itoh et al. have reported that cross-linking of human Fas on WR19L/Fas cells promotes type I cell apoptosis (15), we found that WR/Fas-SM(−) cells are resistant to Fas-mediated apoptosis. Therefore, we used WR/Fas-SM(−) and WR/Fas-SMS1 cells to determine whether membrane SM

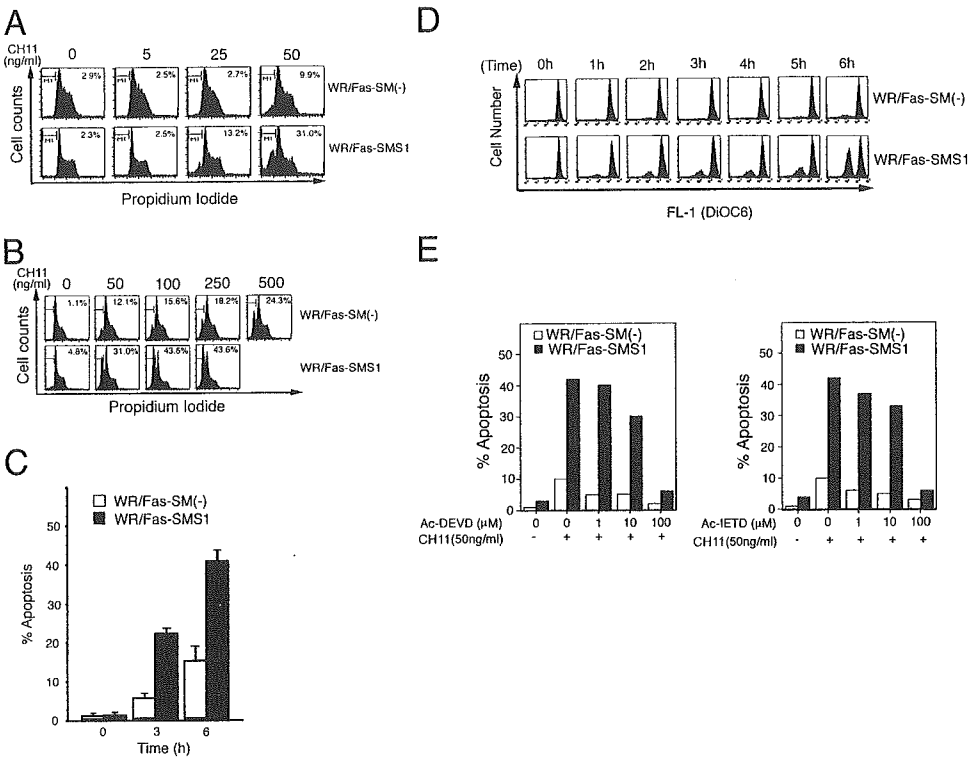

Figure 2. Fas-mediated apoptosis in WR/Fas-SM(−) and WR/Fas-SMS1 cells. (A and B) Dose dependency of Fas-mediated apoptosis. Cells were incubated for 3 h with the indicated concentration of CH11. After incubation, cells were harvested and analyzed by flow cytometry for DNA fragmentation using nuclear staining with PI. The numbers in each box represent the percentages of apoptotic cells. (C) Time kinetics of Fas-mediated apoptosis. Cells were incubated with 50 ng/ml of CH11 for the indicated time, and apoptosis was analyzed by flow cytometry using PI. Error bars represent SEM. (D) Time-kinetics of loss of $\Delta\Psi$m in apoptotic cells. Cells were incubated with 50 ng/ml of CH11 for the indicated time. $\Delta\Psi$m was determined by intracellular staining with $DiOC_6(3)$ and flow cytometry. (E) Inhibition of Fas-mediated apoptosis by caspase inhibitors. Cells were stimulated with 50 ng/ml of CH11 for 6 h in the presence of the indicated amounts of Ac-DEVD-CHO or Ac-IETD-CHO. After incubation, apoptosis was analyzed by flow cytometry using PI.

plays an important role in Fas-mediated apoptosis. Because high antibody concentrations might cause Fas clustering (7), we determined the optimal conditions for Fas-mediated apoptosis by analyzing the effect of concentration of agonistic CH11 (mouse IgM) and the time course of response of these cells. WR/Fas-SMS1 cells underwent stronger apoptosis at 50 ng/ml CH11 than WR/Fas-SM(−) cells, exhibiting 31 and 9.9% apoptosis, respectively (Fig. 2 A). Although apoptosis was increased in a dose-dependent manner in both cells, high concentrations of CH11 (up to 500 ng/ml) induced only 24.3% apoptosis in WR/SMS(−) cells (Fig. 2 B). In subsequent experiments, cells were treated with 50 ng/ml of CH11 as the optimum condition for apoptosis. Next, cells were stimulated with 50 ng/ml CH11 for the indicated time, and WR/Fas-SMS1 cells showed stronger apoptosis compared with WR/Fas-SM(−) cells at both 3 and 6 h (Fig. 2 C).

$\Delta\Psi$m during apoptosis is likely to contribute to the death of the cell through the loss of mitochondrial function before DNA fragmentation in both type I and II cell apoptosis. As shown in Fig. 2 D, the treatment of WR/Fas-SMS1 cells with CH11 dramatically induced a loss of $\Delta\Psi$m as determined by staining with $DiOC_6(3)$, a dye taken up by mitochondria, with similar time kinetics as Fas-mediated apoptosis. However, A majority of WR/Fas-SM(−) cells exhibited a normal $\Delta\Psi$m through the assay (Fig. 2 D). The time kinetics of loss of $\Delta\Psi$m were comparable to those of apoptosis.

Next, we examined whether Fas-mediated apoptosis of WR/Fas-SM(−) and WR/Fas-SMS1 cells depends on caspase activation. Cells were stimulated with 50 ng/ml CH11 for 6 h in the presence of the specific caspase-3 inhibitor (Ac-DEVD-CHO) or the specific caspase-8 inhibitor (Ac-IETD-CHO). As shown in Fig. 2 E, 100 μM of each inhibitor completely suppressed Fas-mediated apoptosis of WR/Fas-SMS1 cells.

Fas-mediated caspase-3 activation of WR/Fas-SM(−) and WR/Fas-SMS1 cells

Cells were stimulated with 50 ng/ml CH11 for the indicated time (Fig. 3 A) and at the indicated concentration for 30 min (Fig. 3 B). Western blot analysis using a caspase-3–specific antibody revealed that the active fragments (p17) of caspase-3 cleaved from 32-kD pro–caspase-3 was expressed at a

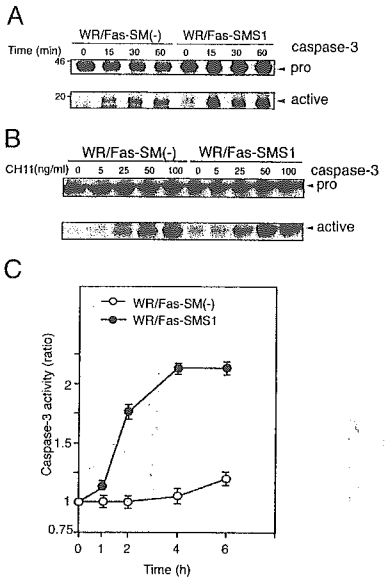

Figure 3. Fas-mediated caspase-3 activation in WR/Fas-SM(−) and WR/Fas-SMS1 cells. Time kinetics (A) and dose dependency (B) of caspase-3 activation by Western blot analysis. Cells were stimulated with 50 ng/ml CH11 for the indicated time (A), or stimulated with the indicated concentration of CH11 for 15 min (B). Total cell lysates were analyzed by Western blot using mouse mAb to caspase-3. The arrows indicate the bands corresponding to 32 kD for procaspase-3 (pro) and 17 kD for the active caspase (active). (C) Cells were stimulated with 50 ng/ml CH11 for the indicated time, and caspase-3 activities were measured in extracts of cell lysates using colorimetric assay kits. Each experiment was done in triplicate. Data are representative of five independent experiments. Error bars represent SEM.

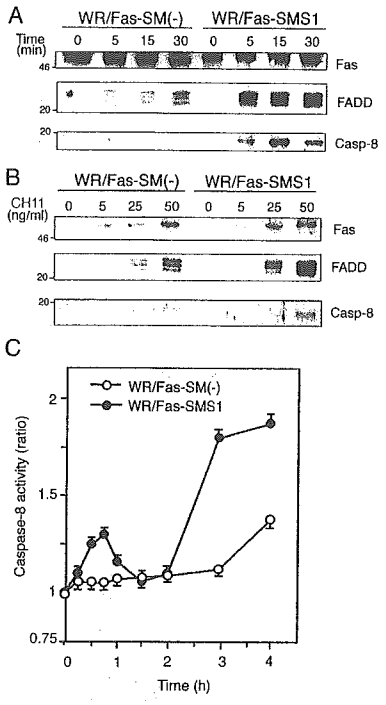

Figure 4. Fas-mediated DISC formation and caspase-8 activation in WR/Fas-SM(−) and WR/Fas-SMS1 cells. Time kinetics (A) and dose dependency (B) of Fas-mediated DISC formation. 2×10^7 cells were stimulated with 50 ng/ml CH11 for the indicated time (A) or stimulated for 15 min with the indicated concentration of CH11 (B). After stimulation, Fas was immunoprecipitated with anti-mouse IgM antibody from Brij 97 lysates. Immunoprecipitates were subjected to 12% SDS-PAGE and immunoblotted with anti-Fas death domain (3D5), anti-FADD, and anti-caspase-8 mAb. Data are representative of five independent experiments. (C) Fas-mediated activation of caspase-8. Cells were stimulated with 50 ng/ml CH11 for the indicated time, and caspase-8 activities were measured in extracts of cell lysates using colorimetric assay kits. Each experiment was done in triplicate. Data are representative of five independent experiments. Error bars represent SEM.

higher level in WR/Fas-SMS1 cells compared with WR/Fas-SM(−) cells in time-dependent (Fig. 3 A) and concentration of Fas antibody–dependent manners (Fig. 3 B). As shown in Fig. 3 C, colorimetric assay revealed that cytoplasmic caspase-3 activity of WR/Fas-SMS1 cells increased more than twofold over baseline by Fas cross-linking. However, caspase-3 activity of WR/Fas-SM(−) cells remained at baseline for the entire 6 h.

Fas-mediated DISC formation and caspase-8 activation in WR/Fas-SM(−) and WR/Fas-SMS1 cells

According to the current model of type I apoptosis, binding of either the FasL or an agonistic antibody induces aggregation of Fas followed by a conformational change in its cytoplasmic domain that results in formation of the DISC (2, 3, 18). Therefore, we examined DISC formation in WR/Fas-SM(−) and WR/Fas-SMS1 cells. Cells were stimulated with 50 ng/ml CH11 for the indicated time (Fig. 4 A) and at the indicated concentration (Fig. 4 B) for 30 min. After lysis, Fas was immunoprecipitated with anti–mouse IgM antibody, and precipitated proteins were examined by immunoblotting with anti-FADD or anti–caspase-8 antibody. The results of the time course study revealed that FADD associated with Fas within 5 min in both cells. However, the association of FADD and Fas in WR/Fas-SMS1 cells was stronger and sooner (with the maximum association at 5 min) than in WR/Fas-SM(−) cells, in which the association gradually increased over the 30-min period. Caspase-8 appeared within the DISC in WR/Fas-SMS1 cells after 5 min of stimulation and reached maximum levels at 15 min. However, caspase-8 within DISC in WR/Fas-SM(−) cells was barely detectable throughout the assay (Fig. 4 A). The results of a dose-dependent experiment revealed that association of FADD and caspase-8 with Fas in WR/Fas-SMS1 cells appeared much stronger than in WR/Fas-SM(−) cells at any concentration of antibody (Fig. 4 B). Although FADD was detected in the DISC after stimulation with 5 ng/ml CH11 in both cell types, caspase-8 appeared in the DISC at a relatively high concentration of CH11; i.e., 25 ng/ml for WR/Fas-SMS1 and 50 ng/ml for WR/Fas-SM(−) cells, respectively (Fig. 4 B).

We also examined the cytoplasmic caspase-8 activity in WR/Fas-SM(−) and WR/Fas-SMS1 cells after Fas cross-linking by colorimetric assay. Interestingly, caspase-8 activities in WR/Fas-SMS1 cells exhibited a biphasic peak after stimulation: the first small peak appeared within 1 h; and the second high peak, after 2 h. However, caspase-8 activity in WR/Fas-SM(−) cells remained at baseline for 3 h, with slight increase at 4 h (Fig. 4 C).

Fas aggregation and capping in WR/Fas-SM(−) and WR/Fas-SMS1 cells

It has been reported that Fas, as well as TNFR, assemble into trimers in the absence of ligands (19, 20). Although Fas trimers do not trigger apoptosis in the resting condition, clustering of these trimers is crucial for Fas-mediated apoptosis (18, 21). CH11 causes the formation of Fas multimers, thereby inducing complete cellular activation leading to capping. Kamitani et al. reported that cross-linking of Fas on the cell surface by CH11 resulted in the formation of high molecular mass Fas aggregates, which were stable in 2% SDS and 5% β-mercaptoethanol (22). As shown in Fig. 5, stimulation with CH11 induced the formation of SDS- and 2-ME–stable, high molecular aggregates (>200 kD) of Fas in both cells, as reported by others (22, 23). Fas aggregates appeared more strongly in WR/Fas-SMS1 cells compared with WR/Fas-SM(−) cells in time-dependent (Fig. 5 A) and CH11 dose–dependent (Fig. 5 B) fashions.

We used confocal microscopy to examine Fas capping on the plasma membrane of WR/Fas-SM(−) and WR/Fas-SMS1 cells after treatment with 50 ng/ml CH11 as described in Materials and methods. In unstimulated cells, Fas was diffusely distributed across the surface on both WR/Fas-SM(−) and WR/Fas-SMS1 cells (Fig. 5 C, 0 min). Cross-linking of Fas with antibody induced small patches of Fas along the plasma membrane, which appeared to fuse to large clusters/capping in WR/Fas-SMS1 cells (Fig. 5 C, 30 min). The frequency of Fas capping on WR/Fas-SMS1 cells was significantly greater than that of WR/Fas-SM(−) cells at each time point ($P < 0.01$; Fig. 5 D).

Fas distribution in lipid rafts of WR/Fas-SM(−) and WR/Fas-SMS1 cells

Recent studies have shown that rafts play an important role in signal transduction pathways, including apoptosis and, in particular, through the organization of surface receptors, signaling enzymes, and adaptor molecules into rafts (5, 24). Muppidi et al. have reported that translocation of Fas into lipid rafts increased sensitivity to Fas-mediated apoptosis (25). To determine Fas distribution of WR/Fas-SM(−) and WR/Fas-SMS1 cells, rafts were isolated using equilibrium

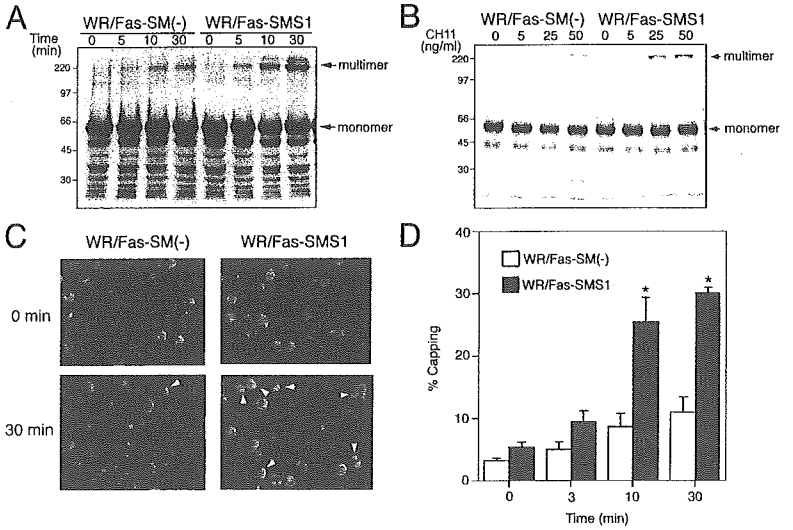

Figure 5. Fas clustering and capping in WR/Fas-SM(−) and WR/Fas-SMS1 cells. Time kinetics (A) and dose dependency (B) of Fas multimer formation. 4×10^7 cells were stimulated with 50 ng/ml CH11 for the indicated time (A), or stimulated for 10 min with the indicated concentration of CH11 (B). After stimulation, cell pellets were snap frozen and treated at 45°C for 1 h in 300 μl of a 1% NP-40–treating solution. DNA in the samples was sheared with a 25-gauge needle, and solubilized samples were loaded on 12% SDS-PAGE. Fas multimers were detected with antibody to the intracellular death domain of human Fas (3D5). Data are representative of more than three independent experiments. (C) Activation-induced capping of Fas. Cells were stained for 20 min with 50 ng/ml CH11 at 4°C. Afterwards, capping was induced by warming cells to 37°C for 30 min in a water bath with mild agitation. Cells were harvested at the indicated times and fixed with 4% paraformaldehyde for 20 min at 22°C. Fixed cells were washed twice and mounted in FITC-conjugated secondary antibody. Fluorescence was detected using a confocal microscope equipped with a SPOT digital camera. The data are representative of more than five experiments. Arrowheads indicate Fas capping. (D) Time kinetics of activation-induced Fas capping. Capping was induced for the indicated time, and cells with Fas clustering were counted by two independent observers. Percentages of capping were calculated in 150–200 total cells. These results are the mean of three independent experiments. Error bars represent SEM. *, $P < 0.01$.

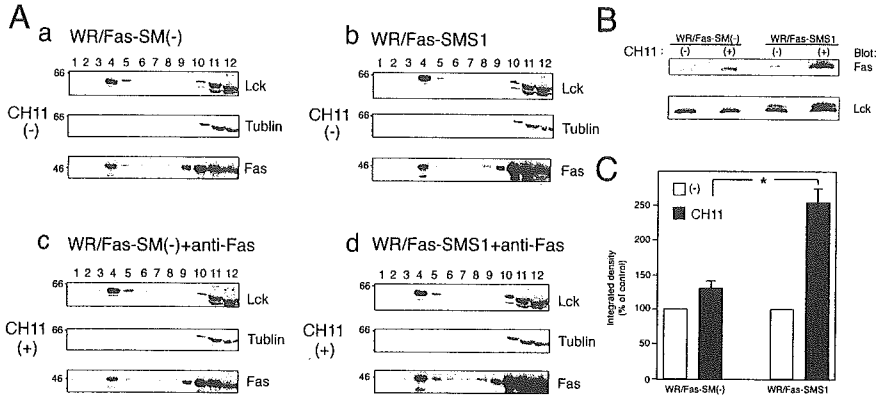

Figure 6. Distribution of Fas into lipid rafts of WR/Fas-SM(−) and WR/Fas-SMS1 cells. (A) 10^8 cells were left unstimulated (a and b) or were stimulated with CH11 for 30 min (c and d), and Triton X-100 lysates were subjected to sucrose density gradient fractionation. Fractions were run on 15% SDS-PAGE and immunoblotted with antibodies against *lck* (a marker for the raft fractions), tublin (a marker for the nonraft fractions), and Fas (3D5). The blots shown are representative of four independent experiments. (B) Redistribution of Fas into lipid rafts on stimulation. Raft fractions (fraction 4) were run on 15% SDS-PAGE and immunoblotted with antibodies against *lck* and Fas. (C) Quantification of Fas contents in lipid rafts was performed densitometrically and normalized to the amount of *lck*. Data are expressed as the mean ± SEM for relative increase of three independent experiments. *, $P < 0.01$.

sucrose density gradients. The position of the membrane rafts in the sucrose gradient was determined by the presence of *lck*, a well-established raft-associated molecule. As shown in Fig. 6, *lck* was enriched in the upper part of the sucrose gradient (fractions 4 and 5), with a secondary localization at the bottom of the gradient in which a cytoskeletal protein, tublin, was localized (fractions 10–12), indicating a separation of the lipid rafts (fractions 4 and 5) from the Triton X-100–soluble membrane. Fas was detected in raft fractions of WR/Fas-SM(−) and WR/Fas-SMS1 cells before stimulation (Fig. 6 A, a and b). Although a substantial shift of Fas into raft fractions was observed in both cells after stimulation, amounts of Fas in raft fractions were greater in WR/Fas-SMS1 than in WR/Fas-SM(−) cells (Fig. 6 A, a and c vs. Fig. 6 A, b and d). The mean of three independent experiments revealed that Fas redistribution in raft fractions was significantly greater in WR/Fas-SMS1 cells than in those of WR/Fas-SM(−) cells after stimulation ($P < 0.01$; Fig. 6, B and C).

Ceramide generation in lipid rafts of WR/Fas-SM(−) and WR/Fas-SMS1 cells

Ceramide modulates the activity of a large number of proteins, and a role in apoptosis induction has been proposed (26–28). However, the signals that activate the enzyme responsible for ceramide production are not well defined, and the actual contribution of ceramide to the apoptotic response remains poorly understood. It has been reported that ceramide formation is associated with the execution phase of apoptosis as a consequence of processes downstream of the activation of caspases (29, 30). Consistent with this, we observed delayed generation of cytosolic ceramide in WR/Fas-SMS1 compared with WR/Fas-SM(−) cells after a 2-h Fas stimulation (unpublished data). However, stress-induced SM hydrolysis occurs rapidly, suggesting that the early event is located in close proximity to the plasma membrane. Recently, it has been reported that aSMase translocates into rafts within minutes after cell stimulation and catalyzes the formation of ceramide from SM (11, 31, 32). Therefore, we analyzed membrane ceramide within lipid rafts in WR/Fas-SM(−) and WR/Fas-SMS1 cells. Although WR/Fas-SM(−) cells, because of a lack of SM synthase, contain more ceramide than WR/Fas-SMS1 cells, both cells showed a similar distribution of ceramide among fractions (Fig. 7 A). Thus, in both cell types, 70% of ceramide is located in raft fractions with ~40% in fraction 4 (Fig. 7 A, bottom). Because membrane SM is one of the major sources of ceramide generation, we next examined Fas-stimulated ceramide generation in raft fractions of WR/Fas-SM(−) and WR/Fas-SMS1 cells. After 5 min of Fas stimulation, cells were lysed, and rafts were isolated using equilibrium sucrose density gradients. Analysis of ceramide in the raft fraction revealed that Fas cross-linking increased ceramide content by 50% in WR/Fas-SMS1 cells (from 2,955 to 4,386 pmol/10^6 cells), but marginally decreased ceramide in WR/Fas-SM(−) cells (from 5,960 to 5,651 pmol/10^6 cells; Fig. 7 B). The mean of three independent experiments revealed that ceramide contents of raft fractions in WR/Fas-SMS1 cells were significantly greater than those of WR/Fas-SM(−) cells ($P < 0.01$; Fig. 7 C).

Effects of exogenous ceramide on Fas-mediated apoptosis in WR/Fas-SM(−) and WR/Fas-SMS1 cells

We and others have shown that ceramide is a proapoptotic lipid mediator because diverse mechanisms of cell stress, including CH11 cross-linking, TNF-α treatment, irradiation, heat shock, and anticancer drugs, increases intracellular ceramide during the execution phase of apoptosis (27, 28, 31, 33–37). It has been reported that the addition of natural or

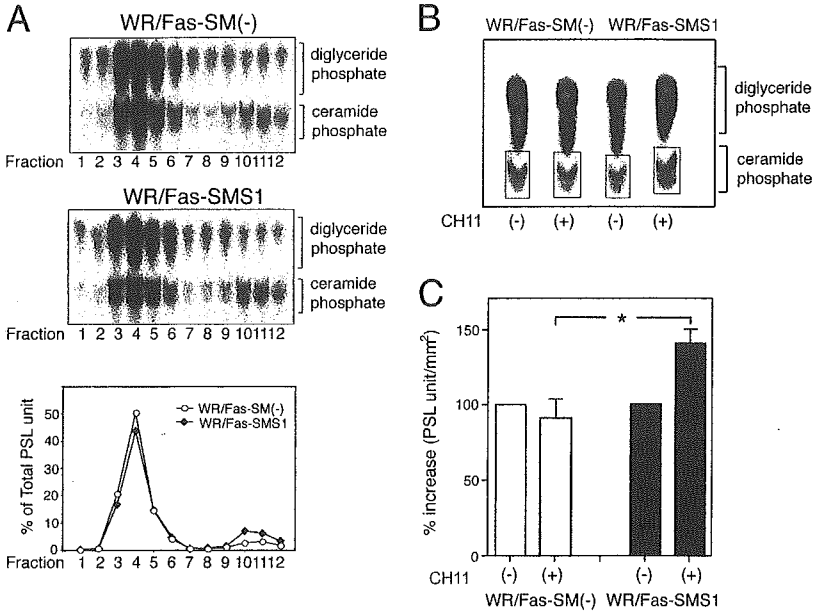

Figure 7. Ceramide generation in lipid rafts of WR/Fas-SM(−) and WR/Fas-SMS1 cells. (A) Ceramide contents in membrane fractions of sucrose density gradient fractionation. 10^8 cells were lysed in Triton X-100 buffer and subjected to sucrose density gradient fractionation. Lipids of each fraction were extracted by the method of Bligh and Dyer (reference 53), and ceramide content was measured by the diacylglycerol kinase assay. After separation of ceramide-1-phosphates by TLC, radioactivity was visualized and estimated. The results are representative of three independent experiments and expressed as the percentage of total PSL arbitrary units. (B) Fas-mediated ceramide generation in lipid rafts. 10^8 cells were left unstimulated or were stimulated with CH11 for 5 min and Triton X-100 lysates were subjected to sucrose density gradient fractionation. Lipids of raft fraction (fraction 4) were extracted by the method of Bligh and Dyer, and ceramide generation was measured by the diacylglycerol kinase assay. Radioactivity was visualized and estimated. The results are representative of three independent experiments. (C) The mean of three independent experiments revealed that ceramide contents of lipid rafts in WR/Fas-SMS1 cells were significantly greater than those of WR/Fas-SM(−) cells. The results were the mean of three independent experiments and expressed as the percentage increase of PSL arbitrary units. Error bars represent SEM. *, $P < 0.01$.

C16-ceramide, which by themselves did not induce apoptosis, enabled soluble FasL to cap and completely restore the apoptosis in aSMase$^{-/-}$ hepatocytes (10, 11, 38). Therefore, we examined the effects of exogenous natural or C16-ceramide on Fas-mediated apoptosis and the formation of Fas multimers in WR/Fas-SM(−) and WR/Fas-SMS1 cells. Cells were pretreated with the indicated concentration of natural or C16-ceramide for 1 h. After washing, cells were stimulated with 50 ng/ml of agonist CH11 for 6 h before assaying for apoptosis, or 30 min before assessing Fas multimer formation. Although natural and C16-ceramide did not induce apoptosis by themselves, both ceramides enhanced Fas-induced apoptosis. However, high concentrations of ceramides, even at 5 μM, could not restore apoptosis of WR/Fas-SM(−) cells to the levels of WR/Fas-SMS1 cells (Fig. 8, A and B). We also examined the effects of natural or C16-ceramide on Fas multimer formation and found that pretreatment of cells with 5 μM natural or C16-ceramides did not enhance Fas multimer formation in WR/Fas-SM(−) and WR/Fas-SMS1 cells (unpublished data).

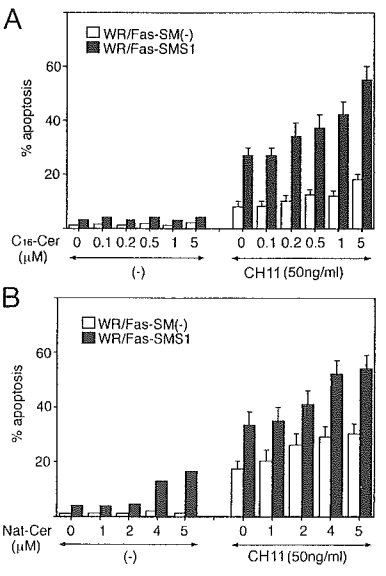

Figure 8. Effects of exogenous ceramides on Fas-mediated apoptosis in WR/Fas-SM(−) and WR/Fas-SMS1 cells. Cells were pretreated with the indicated concentration of C16- (A) or natural (B) ceramide for 1 h. After washing, cells were stimulated with 50 ng/ml CH11 for 6 h and apoptosis was analyzed by flow cytometry using PI. Error bars represent SEM.

DISCUSSION

Currently, two distinct pathways are proposed in Fas-mediated apoptosis signaling; i.e., type I and type II apoptosis. The

consensus in type I apoptosis is that FasL, itself a homotrimer, engages three Fas monomers, leading to the assembly of a trimeric Fas receptor. This FasL-induced trimerization has been suggested to bring together death domains present in the cytoplasmic region of each Fas monomer, leading to a DISC formation. However, it has been reported that soluble FasL (sFasL) reduced apoptosis by <1,000-fold compared with membrane-bound FasL (39), and that sFasL or antibodies to Fas cause cell death more efficiently if polymerized by adsorption on plastic or by molecular cross-linking (40), suggesting that clustering of Fas is important in Fas-mediated apoptosis. Recently, Fas, as well as TNFR, has been reported to assemble into trimers in the absence of ligands through a preligand assembly domain in the extracellular, amino-terminal region of receptors (19, 41). Moreover, Siegel et al. showed that Fas trimers in the absence of FasL do not recruit the DISC, implying a lack of apoptotic signaling (19). Thus, it has been believed that the oligomerization of preassembled Fas trimers is essential for optimal acute signaling and direct activation of the caspase cascade through the DISC (18, 21). However, the molecular basis of Fas clustering is not clear.

It has been reported that Fas ligation triggers translocation of aSMase from an intracellular compartment onto the cell surface, where it hydrolyzes SM to ceramide, and that accumulation of ceramide contributes to transforming small rafts into larger aggregates for signaling platforms, which trap and cluster Fas (7, 10, 11, 31, 42). In contrast to the extensive studies of the acid or neutral SMase in cell death, the biological function of SM synthase has not been elucidated because of a lack of molecular cloning of its responsible genes. Recently, we have succeeded in cloning *SMS1* (12) and established WR/Fas-SM(−) and WR/Fas-SMS1 cells (Fig. 1). Using this system to investigate the mechanisms of Fas-mediated apoptosis, we report here that restoration of membrane SM by transfection of SM synthase gene into SM-deficient cells restored Fas-mediated apoptosis (Fig. 2) through DISC formation (Fig. 4, A and B), activation of caspase-3 (Fig. 3) and caspase-8 (Fig. 4 C), and Fas clustering (Fig. 5). The equivalent expression of other lipid components in the plasma membrane, such as ganglioside GM1 and cholesterol (Fig. 1 C), and equivalent localization of raft fractions in sucrose density gradients (Fig. 6) argue against other lipid abnormalities in SM-deficient cells.

Because lipid rafts promote efficient formation of receptor-associated signaling complexes to produce the biological outcomes dictated by these complexes (24, 43–45), redistribution of Fas in lipid rafts is one possible mechanism for regulating the efficiency of Fas signaling. After titration of Triton X-100 for the isolation of lipid rafts (Fig. S1, available at http://www.jem.org/cgi/content/full/jem.20041685/DC1), we examined whether the redistribution of Fas in lipid rafts is different between WR/Fas-SM(−) and WR/Fas-SMS1 cells. Although Fas cross-linking enhanced redistribution of Fas into raft fractions in both cells, Fas contents in raft fractions were greater in WR/Fas-SMS1 than WR/Fas-SM(−) cells (Fig. 6). These results suggest that membrane SM plays a crucial role for raft partitioning of Fas, which is one of the important mechanisms in Fas-mediated apoptosis of these cells.

It has been believed that the trapping and clustering of Fas may promote the formation of multimers, which ultimately transmit a strong signal into the cell that induces apoptosis (18, 21). We examined the efficiency of Fas clustering in WR/Fas-SM(−) and WR/Fas-SMS1 cells and found that the aggregation and clustering of Fas in WR/Fas-SMS1 cells were markedly enhanced after Fas cross-linking compared with that in WR/Fas-SM(−) cells (Fig. 5), suggesting that oligomerization of Fas is crucial for optimal apoptosis signaling. Although the exact mechanisms of platform formation for Fas clustering on the membrane are not clear, it has been reported that aSMase translocates from an intracellular compartment to the extracellular surface of the cell membrane on Fas stimulation, and that translocation of aSMase to SM-rich rafts generates ceramide (11, 42). Therefore, using a diacylglycerol kinase assay, we measured ceramide content in raft fractions of WR/Fas-SM(−) and WR/Fas-SMS1 cells before and after Fas stimulation. Although ceramide generation in WR/Fas-SM(−) cells is not increased by Fas cross-linking, WR/Fas-SMS1 cells showed a 50% increase in ceramide contents in a raft fraction within 5 min after Fas stimulation (Fig. 7). Because it has been reported that ceramide displaces cholesterol from lipid rafts (46) and self-associates within lipid rafts through hydrogen bonding (47), ceramide may provide the driving force that results in the coalescence of microscopic rafts into large-membrane macrodomains (48), indicating that ceramide in rafts serves to form a signaling platform for Fas clustering (7, 49).

Ceramide has been recognized as an important intracellular lipid mediator related to a variety of cell functions, including cell differentiation and apoptosis (27, 28, 31, 33–37, 50). It has also been reported that the addition of exogenous natural or C16-ceramide enabled soluble FasL to cap and completely restored the apoptosis in aSMase$^{-/-}$ hepatocytes (10, 11, 38). Although exogenous ceramides partially enhanced Fas-mediated apoptosis, they could neither restore apoptosis nor enhance Fas multimer formation in WR/Fas-SM(−) cells to the levels in WR/Fas-SMS1 cells (Fig. 8). In this regard, Liu et al. have reported that IL-1β induced the loss of a resident population of SMs from the SM-rich plasma membrane (i.e., lipid rafts) and the concomitant appearance of ceramide (51). Therefore, we hypothesize that intact SM-enriched membrane domains may be essential for local ceramide production that compartmentalize lipid rafts to ceramide-enriched membrane platforms, leading to Fas capping.

Concerning the molecular ordering of the initial signaling events of CD95, Algeciras-Schimnich et al. have reported four stages: (a) ligand-induced formation of CD95 microaggregates at the cell surface; (b) recruitment of FADD to form a DISC; (c) formation of large CD95 surface clusters, which is positively regulated by DISC-generated caspase-8; and (d)

internalization of activated CD95 through an endosomal pathway (52). We examined caspase-8 activation, ceramide generation within lipid rafts, redistribution of Fas within lipid rafts, and Fas multimer formation at very early time points (Fig. S2, available at http://www.jem.org/cgi/content/full/jem.20041685/DC1). Caspase-8 activation, ceramide generation, and Fas redistribution within lipid rafts were observed within 1 min in WR/Fas-SMS1 but not WR/Fas-SM(−) cells. In contrast, Fas multimer formation was observed in WR/Fas-SMS1 but not WR/Fas-SM(−) cells at later time points (after 2 min; Fig. S2). Thus, our findings support a crucial role for membrane SM in the extrinsic pathway of Fas-mediated apoptosis through the generation of ceramide in lipid rafts, which facilitates efficient Fas clustering, DISC formation, and the early caspase-8 activation leading to the downstream cascade of caspase-3 activation.

MATERIALS AND METHODS

Cells and cell transfection. Mouse T cell lymphoma WR19L cells transfected with the cDNA for the human *Fas* gene (WR19L/Fas; reference 15) were a gift of S. Yonehara (Kyoto University, Kyoto, Japan). We isolated the SM-defective WR/Fas-SM(−) cells and the SM-containing WR/Fas-SM(+) cells from the original WR19L/Fas cells by limiting dilution. *SMS1*, subcloned into the pLIB expression vector, was transfected into the WR/Fas-SM(−) cells in VSV-G retroviral particles. These cells were designated WR/Fas-SMS1 cells (12).

Antibodies and reagents. Anti-Fas (CH11, mouse IgM) and anti-FADD (1F7, mouse IgG1) were purchased from MBL International Corporation. FITC-conjugated anti–mouse IgM, anti–mouse IgG2a, anti–human Fas (DX2), and anti–caspase-3/CPP32 pAb were purchased from BD Biosciences. Anti-Fas death domain (3D5) and anti–caspase-8 (1G12) antibodies were purchased from Qbiogene. Lysenin, FITC-conjugated CTx, peroxidase-conjugated CTx, and methyl-β-cyclodextrin were purchased from Sigma-Aldrich. Rabbit anti–mouse IgG mAb was purchased from Cappel. Ac-DEVD-CHO and Ac-IETD-CHO were purchased from Peptide Institute. RNase and saponin were purchased from Nacalai Tesque. The cell viability assay kit using WST-8 (2-(2-methoxy-4-nitrophenyl)-3-(4-nitrophenyl)-5-(2,4-disulfophenyl)-2H-tetrazolium) was purchased from Wako Co. Ltd. L-[^{14}C]serine and γ-[^{32}P]ATP were purchased from GE Healthcare. Rabbit anti–mouse IgM (μ chain specific) antibody was purchased from Zymed Laboratories. The ECL immunodetection system and horseradish peroxidase–conjugated goat anti–mouse or anti–rabbit IgG mAb were obtained from GE Healthcare.

FACS analysis. DNA fragmentation was quantified by analyzing cell cycle and total DNA content to measure cell death by apoptosis. In brief, cells were treated with CH11 at the indicated concentration and incubated for the indicated time shown in the figures. After harvesting, cells were resuspended in permeabilization solution (0.5% paraformaldehyde and 0.5% saponin) and treated with 50 μg/ml RNase A for 30 min at room temperature, and propidium iodide (PI; Molecular Probes) was added to a final concentration of 20 μg/ml. After 20 min, the fluorescence of the PI-stained DNA was quantitated on a per cell basis using a FACSCalibur (BD Biosciences), and cells with subdiploid content were considered to be apoptotic cells.

To detect SM localized at the outer leaflet of the plasma membrane, cells were stained on ice for 30 min with nontoxic lysenin–MBP (16), incubated for 30 min with FITC-conjugated anti–mouse IgG (Sigma-Aldrich), and analyzed with a FACSCalibur. Surface expression of ganglioside GM1 and cholesterol was analyzed using FITC-conjugated CTx) or fPEG-cholesterol (17), respectively. Data were analyzed using CellQuest software (Becton Dickinson).

To assess $\Delta\Psi$m, healthy or dying cells were incubated for 15 min at 37°C in buffer containing 40 nM 3,3′-dihexyloxacarbocyanine iodide ($DiOC_6(3)$; Molecular Probes) before the addition of 5 μg/ml PI. After compensation to exclude nonviable cells, fluorescence was recorded at 525 nM (FL-1) for $DiOC_6(3)$ and 600 nM (FL-3) for PI on a FACScan (26).

Confocal microscopy. To assess Fas capping, cells were stained for 20 min with 50 ng/ml of CH11 at 4°C, and capping was induced by warming cells to 37°C in a water bath with mild agitation. Cells were harvested at the indicated times shown in the figures and fixed with 4% paraformaldehyde for 10 min at 22°C. Fixed cells were washed twice and mounted in FITC-conjugated secondary antibody. Fluorescence was detected with a confocal microscope (LSM-5 Pascal; Carl Zeiss MicroImaging, Inc.) equipped with a SPOT digital camera. Large clusters of Fas were defined as cells in which the fluorescence condenses onto >25% of the cell surface, whereas fluorescence was homogeneously distributed on the membrane of resting cells.

For visualization of SM localized at the outer leaflet of the plasma membrane, cells were allowed to settle onto slides coated with poly-L-lysine, fixed in 4% formaldehyde, stained with lysenin–MBP at 4°C for 45 min, and treated with anti-MBP.

Cell labeling and lipid separation. The method for detection of SM synthesis is described elsewhere (28). In brief, cells were reseeded at 5×10^5 cells/ml in RPMI 1640 with 2% FBS and L-[^{14}C]serine (specific activity, 155 mCi/mmol) and incubated at 37°C in 5% CO_2 for 36 h. The cell lipids were extracted by the method of Bligh and Dyer (53), applied on silica gel TLC plate (Whatman), and developed with solvent containing methyl acetate/propanol/chloroform/methanol/0.25% KCl (25:25:25:10:9). The radioactive spots were visualized and quantified using an image analyzer (BAS 2000; Fuji Photo Film).

Immunoprecipitation, Western blotting, and immunoblotting. Cells were solubilized with lysis buffer containing 50 mM Tris-HCl, pH 7.6, 1% Brij 97, 300 mM NaCl, 5 mM EDTA, 10 μg/ml leupeptin, 10 μg/ml aprotinin, 1 mM PMSF, and 1 mM sodium orthovanadate with gentle rocking for 30 min at 4°C. Immunoprecipitated proteins were eluted by boiling in SDS-containing sample buffer and fractionated by SDS-PAGE (8–12% polyacrylamide gels; reference 54). Proteins were electrophoretically transferred to polyvinylidene difluoride (Immobilon-P) membranes (Sigma-Aldrich). Peroxidase-conjugated secondary antibodies (GE Healthcare) were used at a 1:1,000 dilution, and immunoreactive bands were visualized using ECL. Densitometry of the protein bands was performed using National Institutes of Health image software (55). Quantitation of Fas in raft fractions was corrected to the amount of *lck*.

The aggregated form of Fas was detected by the method of Kamitani et al. (22). In brief, cell pellets were snap frozen to prevent protein degradation. Frozen pellets were treated at 45°C for 1 h in 300 ml of 2% treating solution containing 5% β-mercaptoethanol. DNA in the samples were sheared with a 25-gauge needle, and solubilized samples were loaded on 12% SDS-PAGE. Aggregated Fas was detected by 3D5, a mouse mAb (IgG1) specific for the intracellular death domain of human Fas (Qbiogene).

Caspase activity assay. Activities of caspase-3 and -8 were determined using a colorimetric assay kit (MBL International Corporation) according to the manufacturer's protocol. Apoptosis inhibition was assayed in cells stimulated for 6 h with 50 ng/ml CH11 in the presence of the indicated doses of Ac-DEVD-CHO or Ac-IETD-CHO shown in the figures.

Isolation of a raft fraction in equilibrium density gradients. Raft fractions were prepared as described by Rodgers and Rose (56) with minor modifications (8). In brief, 10^8 cells were lysed with 1 ml MS-buffered saline (MBS; 25 mM MES, pH 6.5, and 150 mM NaCl) containing 1% Triton X-100, 10 μg/ml aprotinin, 10 μg/ml leupeptin, 1 mM PMSF, 1 mM sodium orthovanadate, and 5 mM EDTA. The lysate was homogenized

with 20 strokes of a Dounce homogenizer (Iwaki Glass Co.), gently mixed with an equal volume of 80% sucrose (wt/vol) in MBS, and placed in the bottom of a 14 × 95 mm clear centrifuge tube (model 344060; Beckman Coulter). The sample was then overlaid with 6.5 ml of 30% sucrose and 3.5 ml of 5% sucrose in MBS and centrifuged at 200,000 *g* in a rotor (model SW40Ti; Beckman Coulter) at 4°C for 16 h. After centrifugation, 12 1-ml fractions (excluding the pellet) were collected from the top of the gradient.

Ceramide measurement. Lipids were extracted from cell lysates by the method of Bligh and Dyer (53), and ceramide mass measurement using *Escherichia coli* diacylglycerol kinase, which phosphorylates ceramide to ceramide-1-phosphate, was performed as described previously (50). The solvent system to separate ceramide-1-phosphate and phosphatidic acid on TLC plates consists of chloroform/acetone/methanol/acetic acid/H_2O (10:4:3:2:1). Radioactivity within spots of ceramide-1-phosphate was estimated with an image analyzer system (BASE III; Fuiji) and expressed as PSL arbitrary units (54), and ceramide levels were corrected for phospholipid phosphate as described elsewhere (57).

Statistical analysis. Statistical significance was evaluated by unpaired *t* tests and by analysis of variance as applicable; $P < 0.01$ was considered statistically significant.

Online supplemental material. Fig. S1 shows concentration of Triton X-100 for lipid raft separation. Fig. S2 shows early timecourse of caspase-8 activity, ceramide generation in lipid rafts, Fas redistribution into lipid rafts, and Fas multimer formation. Online supplemental material is available at http://www.jem.org/cgi/content/full/jem.20041685/DC1.

We thank Drs. H. Inoue and S. Goda of Osaka Dental University for technical assistance.

This work was supported by grants 13557160, 15024236, and 15390313 (to H. Umehara) from the Japanese Ministry of Education and Science and Culture, by the Uehara Memorial Foundation, and by grant P04244 (to Z.-X. Jin) from the Japan Society for the Promotion of Science.

The authors have no conflicting financial interests.

Submitted: 19 August 2004
Accepted: 2 May 2005

REFERENCES

1. Marsden, V.S., and A. Strasser. 2003. Control of apoptosis in the immune system: Bcl-2, BH-3 only proteins and more. *Annu. Rev. Immunol.* 21:71–105.
2. Scaffidi, C., S. Fulda, A. Srinivasan, C. Friesen, F. Li, K.J. Tomaselli, K.M. Debatin, P.H. Krammer, and M.E. Peter. 1998. Two CD95 (APO-1/Fas) signaling pathways. *EMBO J.* 17:1675–1687.
3. Wajant, H. 2002. The Fas signaling pathway: more than a paradigm. *Science.* 296:1635–1636.
4. Hengartner, M.O. 2000. The biochemistry of apoptosis. *Nature.* 407: 770–776.
5. Simons, K., and E. Ikonen. 1997. Functional rafts in cell membranes. *Nature.* 387:569–572.
6. Brown, D.A., and E. London. 1998. Functions of lipid rafts in biological membranes. *Annu. Rev. Cell Dev. Biol.* 14:111–136.
7. Grassme, H., A. Jekle, A. Riehle, H. Schwarz, J. Berger, K. Sandhoff, R. Kolesnick, and E. Gulbins. 2001. CD95 signaling via ceramide-rich membrane rafts. *J. Biol. Chem.* 276:20589–20596.
8. Inoue, H., O. Yoneda, Y. Minami, Y. Tanaka, T. Okazaki, H. Imai, E. Bloom, N. Domae, and H. Umehara. 2002. Lipid rafts as the signaling scaffold for NK cell activation: tyrosine phosphorylation and association of LAT with PI 3-kinase and PLC-γ following CD2 stimulation. *Eur. J. Immunol.* 32:2188–2198.
9. Delmas, D., C. Rebe, S. Lacour, R. Filomenko, A. Athias, P. Gambert, M. Cherkaoui-Malki, B. Jannin, L. Dubrez-Daloz, N. Latruffe, and E. Solary. 2003. Resveratrol-induced apoptosis is associated with Fas redistribution in the rafts and the formation of a death-inducing signaling complex in colon cancer cells. *J. Biol. Chem.* 278:41482–41490.
10. Cremesti, A., F. Paris, H. Grassme, N. Holler, J. Tschopp, Z. Fuks, E. Gulbins, and R. Kolesnick. 2001. Ceramide enables Fas to cap and kill. *J. Biol. Chem.* 276:23954–23961.
11. Grassme, H., A. Cremesti, R. Kolesnick, and E. Gulbins. 2003. Ceramide-mediated clustering is required for CD95-DISC formation. *Oncogene.* 22:5457–5470.
12. Yamaoka, S., M. Miyaji, T. Kitano, H. Umehara, and T. Okazaki. 2004. Expression cloning of a human cDNA restoring sphingomyelin synthesis and cell growth in sphingomyelin synthase-deficient cells. *J. Biol. Chem.* 279:18688–18693.
13. Huitema, K., J.V.D. Dikkenberg, J.F. Brouwers, and J.C. Holhuis. 2004. Identification of a family of animal sphingomyelin synthases. *EMBO J.* 23:33–44.
14. Yamaji, A., Y. Sekizawa, K. Emoto, H. Sakuraba, K. Inoue, H. Kobayashi, and M. Umeda. 1998. Lysenin, a novel sphingomyelin-specific binding protein. *J. Biol. Chem.* 273:5300–5306.
15. Itoh, N., S. Yonehara, A. Ishii, M. Yonehara, S. Mizushima, M. Sameshima, A. Hase, Y. Seto, and S. Nagata. 1991. The polypeptide encoded by the cDNA for human cell surface antigen Fas can mediate apoptosis. *Cell.* 66:233–243.
16. Yamaji-Hasegawa, A., A. Makino, T. Baba, Y. Senoh, H. Kimura-Suda, S.B. Sato, N. Terada, S. Ohno, E. Kiyokawa, M. Umeda, and T. Kobayashi. 2003. Oligomerization and pore formation of a sphingomyelin-specific toxin, lysenin. *J. Biol. Chem.* 278:22762–22770.
17. Sato, S.B., K. Ishii, A. Makino, K. Iwabuchi, A. Yamaji-Hasegawa, Y. Senoh, I. Nagaosa, H. Sakuraba, and T. Kobayashi. 2004. Distribution and transport of cholesterol-rich membrane domains monitored by a membrane-impermeant fluorescent polyethylene glycol-derivatized cholesterol. *J. Biol. Chem.* 279:23790–23796.
18. Mundle, S.D., and A. Raza. 2002. Defining the dynamics of self-assembled Fas-receptor activation. *Trends Immunol.* 23:187–194.
19. Siegel, R.M., J.K. Frederiksen, D.A. Zacharias, F.K.M. Chan, M. Johnson, D. Lynch, R.Y. Tsien, and M. Lenardo. 2000. Fas preassociation required for apoptosis signaling and dominant inhibition by pathogenic mutations. *Science.* 288:2354–2357.
20. Chan, F.K.M., H.J. Chun, L. Zheng, R.M. Siegel, K.L. Bui, and M.J. Lenardo. 2000. A domain in TNF receptors that mediates ligand-independent receptor assembly and signaling. *Science.* 288:2351–2354.
21. Golstein, P. 2000. FasL binds preassembled Fas. *Science.* 288:2328–2329.
22. Kamitani, T., H.P. Nguyen, and E.T.H. Yeh. 1997. Activation-induced aggregation and processing of the human Fas antigen. *J. Biol. Chem.* 272:22307–22314.
23. Lee, Y.-J., and E. Shacter. 2001. Fas aggregation does not correlate with Fas-mediated apoptosis. *J. Immunol.* 167:82–89.
24. Dykstra, M., A. Cherukuri, H.W. Sohn, S.J. Tzeng, and S.K. Pierce. 2003. Location is everything: lipid rafts and immune cell signaling. *Annu. Rev. Immunol.* 21:457–481.
25. Muppidi, J., and R.M. Siegel. 2004. Ligand-independent redistribution of Fas (CD95) into lipid rafts mediates clonotypic death. *Nat. Immunol.* 5:182–189.
26. Kondo, T., K. Iwai, T. Kitano, M. Watanabe, Y. Taguchi, T. Yabu, H. Umehara, N. Domae, T. Uchiyama, and T. Okazaki. 2002. Control of ceramide-induced apoptosis by IGF-1: involvement of PI-3 kinase, caspase-3 and catalase. *Cell Death Differ.* 9:682–692.
27. Iwai, K., T. Kondo, M. Watanabe, T. Yabu, Y. Taguchi, H. Umehara, A. Takahashi, T. Uchiyama, and T. Okazaki. 2003. Ceramide increases oxidative damage due to inhibition of catalase by caspase-3-dependent proteolysis in HL-60 cell apoptosis. *J. Biol. Chem.* 278:9813–9822.
28. Watanabe, I., T. Kitano, T. Kondo, T. Yabu, Y. Taguchi, M. Tashima, H. Umehara, N. Domae, T. Uchiyama, and T. Okazaki. 2004. Increase of nuclear ceramide through caspase-3-dependent regulation of the "sphingomyelin (SM) cycle" in Fas-induced apoptosis. *Cancer Res.* 64:1000–1007.
29. Tepper, A.D., P. Ruurs, T. Wiedmer, P.J. Sims, J. Borst, and W.J. van Blitterswijk. 2000. Sphingomyelin hydrolysis to ceramide during the execution phase of apoptosis results from phospholipid scrambling and alters cell-surface morphology. *J. Cell Biol.* 150:155–164.

30. Hetz, C.A., M. Hunn, P. Rojas, V. Torres, L. Leyton, and A.F.G. Quest. 2002. Caspase-dependent initiation of apoptosis and necrosis by the Fas receptor in lymphoid cells: onset of necrosis is associated with delayed ceramide increase. *J. Cell Sci.* 115:4671–4683.
31. Blitterswijk, W.J.V., A.H. van der Luit, R.J. Veldman, and J. Borst. 2003. Ceramide: second messenger or modulator of membrane structure and dynamics? *Biochem. J.* 369:199–211.
32. Gulbins, E., and H. Grassme. 2002. Ceramide and cell death receptor clustering. *Biochim. Biophys. Acta.* 1585:139–145.
33. Kolesnick, R., and Z. Fuks. 2003. Radiation and ceramide-induced apoptosis. *Oncogene.* 22:5897–5906.
34. Pettus, B.J., C.E. Chalfant, and Y.A. Hannum. 2002. Ceramide in apoptosis: an overview and current perspective. *Biochim. Biophys. Acta.* 1585:114–125.
35. Sawai, H., T. Okazaki, Y. Takeda, M. Tashima, H. Sawada, M. Okuma, S. Kishi, H. Umehara, and N. Domae. 1997. Ceramide-induced translocation of protein kinase C-delta and -epsilon to the cytosol. *J. Biol. Chem.* 272:2452–2458.
36. Kondo, T., Y. Suzuki, T. Kitano, K. Iwai, M. Watanabe, H. Umehara, N. Daido, N. Domae, M. Tashima, T. Uchiyama, and T. Okazaki. 2002. Vesnarinone causes oxidative damage by inhibiting catalase function through ceramide action in myeloid cell apoptosis. *Mol. Pharmacol.* 61:620–627.
37. Uchida, Y., M. Itoh, Y. Taguchi, S. Yamaoka, M. Umeda, S. Ichikawa, Y. Hirabayashi, W.M. Holleran, and T. Okazaki. 2004. Ceramide reduction and transcriptional up-regulation of glucosylceramide synthase through Doxorubicin-activated Sp1 in drug-resistant HL-60/ADR cells. *Cancer Res.* 64:6271–6279.
38. Paris, F., H. Grassme, A. Cremesti, J. Zager, Y. Fong, A. Haimovitz-Friedman, Z. Fuks, E. Gulbins, and R. Kolesnick. 2001. Natural ceramide reverses Fas resistance of acid sphingomyelinase$^{-/-}$ hepatocytes. *J. Biol. Chem.* 276:8297–8305.
39. Schneider, P., N. Holler, J.-L. Bodmer, M. Hahne, K. Frei, A. Fontana, and J. Tschopp. 1998. Conversion of membrane-bound Fas (CD95) ligand to its soluble form is associated with down-regulation of its proapoptotic activity and loss of liver toxicity. *J. Exp. Med.* 187: 1205–1213.
40. Huang, D.C.S., M. Hahne, M. Schroeter, K. Frei, A. Fontana, A. Villunger, K. Newton, J. Tschopp, and A. Strasser. 1999. Activation of Fas by FasL induces apoptosis by a mechanism that cannot be blocked by Bcl-2 or Bcl-XL. *Proc. Natl. Acad. Sci. USA.* 96:14871–14876.
41. Papoff, G., P. Hausler, A. Eramo, M.G. Pagano, G.D. Leve, A. Signore, and G. Ruberti. 1999. Identification and characterization of a ligand-independent oligomerization domain in the extracellular region of the CD95 death receptor. *J. Biol. Chem.* 274:38241–38250.
42. Gulbins, E., and R. Kolesnick. 2003. Raft ceramide in molecular medicine. *Oncogene.* 22:7070–7077.
43. Cherukuri, A., M. Dykstra, and S.K. Pierce. 2001. Floating the raft hypothesis: Lipid rafts play a role in immune cell activation. *Immunity.* 14: 657–660.
44. Bromley, S.K., W.R. Burack, K.G. Johnson, K. Somersalo, T.N. Sims, C. Sumen, M.M. Davis, A.S. Shaw, P.M. Allen, and M.L. Dustin. 2001. The immunological synapse. *Annu. Rev. Immunol.* 19:375–396.
45. Davis, D.M. 2002. Assembly of the immunological synapse for T cell and NK cells. *Trends Immunol.* 23:356–363.
46. London, M., and L. Erwin. 2004. Ceramide selectively displaces cholesterol from ordered lipid domain (Rafts). *J. Biol. Chem.* 279:9997–10004.
47. Veiga, M.P., J.L.R. Arrondo, F.M. Goni, and A. Alonso. 1999. Ceramides in phospholipid membranes: effects on bilayer stability and transition to nonlamellar phases. *Biophys. J.* 76:342–350.
48. Holopainen, J.M., M. Subramanian, and P.K. Kinnunen. 1998. Sphingomyelinase induces lipid microdomain formation in a fluid phosphatidylcholine/sphingomyelin membrane. *Biochemistry.* 37:17562–17570.
49. Grassme, H., V. Jendrossek, A. Riehle, G. von Kurthy, J. Berger, H. Schwarz, M. Weller, R. Kolesnick, and E. Gulbins. 2003. Host defence against *Pseudomonas aeruginosa* requires ceramide-rich membrane rafts. *Nat. Med.* 9:322–330.
50. Okazaki, T., R.M. Bell, and Y.A. Hannun. 1989. Sphingomyelin turnover induced by vitamin D3 in HL-60 cells. *J. Biol. Chem.* 264: 19076–19080.
51. Liu, P., and R.G. Anderson. 1995. Compartmentalized production of ceramide at the cell surface. *J. Biol. Chem.* 270:27179–27185.
52. Algeciras-Schimnich, A., L. Shen, B.C. Barnhart, A.E. Murmann, J.K. Burkhardt, and M.E. Peter. 2002. Molecular ordering of the initial signaling events of CD95. *Mol. Cell. Biol.* 22:207–220.
53. Bligh, E., and W. Dyer. 1959. A rapid method of total lipid extraction and purification. *Can. J. Biochem. Physiol.* 37:911–917.
54. Umehara, H., J.-Y. Huang, T. Kono, F.H. Tabassam, T. Okazaki, E.T. Bloom, and N. Domae. 1997. Involvement of protein tyrosine kinase p72^{syk} and phosphatidylinositol 3-kinase in CD2-mediated granular exocytosis in natural killer cell line. *J. Immunol.* 159:1200–1207.
55. Umehara, H., J.-Y. Huang, T. Kono, F.H. Tabassam, T. Okazaki, S. Gouda, Y. Nagano, E.T. Bloom, and N. Domae. 1998. Co-stimulation of T cells with CD2 augments TCR-CD3-mediated activation of protein tyrosine kinase p72^{syk}, resulting in increased tyrosine phosphorylation of adapter proteins, Shc and Cbl. *Int. Immunol.* 10:833–845.
56. Rodgers, W., and J.K. Rose. 1996. Exclusion of CD45 inhibits activity of p56^{lck} associated with glycolipid-enriched membrane domains. *J. Cell Biol.* 135:1515–1523.
57. Okazaki, T., A. Bielawska, R.M. Bell, and Y.A. Hannun. 1990. Role of ceramide as a lipid mediator of 1 alpha, 25-dehydroxyvitamin D3-induced HL-60 cell differentiation. *J. Biol. Chem.* 265:15823–15831.

International Immunology, Vol. 17, No. 10, pp. 1327–1336
doi:10.1093/intimm/dxh311

Amelioration of experimental arthritis by a calpain-inhibitory compound: regulation of cytokine production by E-64-d *in vivo* and *in vitro*

Hajime Yoshifuji[1], Hisanori Umehara[2], Hidenori Maruyama[3], Mari Itoh[3], Masao Tanaka[1], Daisuke Kawabata[1], Takao Fujii[1] and **Tsuneyo Mimori[1]**

[1]Department of Rheumatology and Clinical Immunology, Kyoto University Graduate School of Medicine, 54 Shogoin-Kawahara-cho, Sakyo-ku, Kyoto 606-8507, Japan
[2]Division of Hematology and Immunology, Department of Internal Medicine, Kanazawa Medical University, Ishikawa, Japan
[3]Discovery Pharmacology I Group, Pharmacology and Microbiology Research Laboratories, Dainippon Pharmaceutical Co., Ltd, Osaka, Japan

Keywords: anti-type II collagen antibody-induced arthritis, calpastatin, IL-6, rheumatoid arthritis

Abstract

Calpain, a calcium-dependent cysteine proteinase, has been reported to participate in the pathophysiology of rheumatoid arthritis (RA). The aim of this study is to investigate the therapeutic efficacy of calpain-inhibitory compounds in an animal model of RA and to clarify the underlying mechanisms *in vivo* and *in vitro*. Arthritis was induced in BALB/c mice with anti-type II collagen mAbs and LPS, and the mice were treated intra-peritoneally with a high dose (9 mg kg^{-1} per day) or low dose (3 mg kg^{-1} per day) of E-64-d (a membrane-permeable cysteine proteinase inhibitor) or control diluent. As a result, a high dose of E-64-d significantly alleviated the clinical arthritis and the histopathological findings, compared with the control diluent, although a low dose of E-64-d did not have a significant effect. Next, we evaluated the effects of E-64-d on cytokine mRNA expression at the inflamed joints by quantitative reverse transcription–PCR. High dose of E-64-d significantly decreased IL-6 and IL-1β mRNA levels at the inflamed joints. The regulatory effects of E-64-d on cytokine production were also confirmed *in vitro*, using a synovial cell line (E11) and crude synoviocytes derived from RA patients. These results suggest the key roles of calpain in the pathophysiology of arthritis and that calpain-inhibitory compounds might be applicable to the treatment of arthritic diseases such as RA.

Introduction

Rheumatoid arthritis (RA) is a chronic refractory disease, whose main symptom is polyarthritis characterized by autonomous synovial proliferation and osteocartilaginous destruction. Although the pathogenesis of RA remains to be elucidated, studies have indicated the contribution of proteinases, cytokines and auto-antibodies to the progression of the disease. First, over-expression of proteinases such as calpains (1–3), cathepsins (4) and matrix metalloproteinases (MMPs) (5) at the disease-affected joints has been reported and assumed to contribute to the osteocartilaginous destruction. Second, cytokines are now widely recognized to play major roles in RA, since an increasing number of favorable outcomes has been reported in trials to treat RA with biological agents against tumor necrosis factor-α (TNF-α) (6), IL-1 and IL-6. Third, the involvement of various auto-antibodies such as antibodies to citrullinated proteins (7), glucose-6-phosphate isomerase (8) and follistatin-related protein (FRP) (9–11) has been reported in the pathophysiology of RA. For example, we have reported that anti-FRP antibodies were detected in synovial fluids of RA patients (9), and demonstrated that recombinant FRP inhibited the production of MMP-1 and MMP-3 in cultured synoviocytes (10) and ameliorated an animal model of RA (11).

We and another group have identified a new auto-antibody against calpastatin (12, 13), which was detected significantly more frequently in RA patients than in patients with other

Correspondence to: H. Yoshifuji; E-mail: yoshifuj@kuhp.kyoto-u.ac.jp

Transmitting editor: M. Miyasaka

Received 5 February 2005, *accepted* 20 July 2005

Advance Access publication 13 September 2005

rheumatic diseases or in healthy controls (12, 14, 15). Recently, it was reported that sensitivity and specificity of anti-calpastatin antibodies were 83 and 96% for RA, respectively (14). The positivity of anti-calpastatin antibodies was correlated with serological markers of the disease activity or a recent-onset subset in RA patients (15–17).

Calpastatin, an endogenous inhibitor of calpain, is a ubiquitous 70-kDa protein, comprising five domains, L, I, II, III and IV (18). Calpain, a Ca^{2+}-dependent cysteine proteinase, is a ubiquitous enzyme that has two subtypes, μ- and m-calpain, both of which have two subunits of 80 and 28 kDa (18). Calpain exhibits proteinase activity toward a wide range of substrates, such as cytoskeletal proteins, kinases, phosphatases, membrane-associated proteins and transcription factors (18). Since it cleaves the substrates at a limited number of specific sites for their activation or inactivation, calpain is regarded as a 'biomodulator' rather than a digestive enzyme (19). For example, calpain activates IL-1α or protein kinase C by cleaving it (20, 21). Through the modulation of these substrates, calpain is supposed to contribute to the pathophysiology of RA. It is worth mentioning that calpain is more highly expressed in the synovial membranes of RA patients than in those of healthy controls (2), and similarly, calpain is detected in the synovial membranes of mice with collagen (CL)-induced arthritis, while not detected in those of non-manipulated mice (22).

E-64-d (synonyms: loxistatin, ESTand Ep453), a membrane-permeable cysteine proteinase inhibitor, has been used in order to inhibit calpain *in vivo* and *in vitro* (23, 24). In the present study, we examined the therapeutic efficacy of two calpain-inhibitory compounds, E-64-d and recombinant calpastatin (rCS), in mice with anti-type II CL antibody-induced arthritis. We also analyzed the underlying mechanisms *in vivo* and *in vitro*, using the mice with mAb-induced arthritis and a fibroblast-like synovial cell line (E11) or crude synoviocytes of a RA patient.

Methods

Reagents

E-64 [molecular weight (MW) 375.4, non-membrane permeable] and E-64-d (MW 342.4, membrane permeable) were purchased from Amresco (Solon, OH, USA) and Peptide Institute (Osaka, Japan), respectively. *Escherichia coli*-expressed recombinant human calpastatin (14 kDa, identical to domain I) was from Takara Shuzo (Shiga, Japan) and filtrated through an endotoxin cut filter (Zetapore-dispo 020SP, Cuno, Meriden, CT, USA) before use. Phorbol 12-myristate 13-acetate (PMA) and ionomycin (IM) were from Wako Chemicals (Richmond, VA, USA) and EMD Biosciences (La Jolla, CA, USA), respectively.

Induction and treatment of murine arthritis

Institutional bioethical approval (no. 02004, Kyoto University Graduate School of Medicine) was acquired prior to the animal experiments. Arthritis was induced in 7-week-old female BALB/c mice (Japan SLC, Hamamatsu, Japan) with a mixture of anti-type II CL mAbs (Arthrogen-CIA mAb, Chondrex, Redmond, WA, USA) and LPS; according to the method of Terato *et al.* (25). Briefly, 2 mg per body of mAb mixture was injected intra-peritoneally (i.p.) into each mouse (day –2), and 48 h later, 50 μg per body of LPS was injected i.p. in order to enhance the arthritis (day 0). To prevent the development of the disease, a high dose (9 mg kg^{-1} per day) or low dose (3 mg kg^{-1} per day) of E-64-d, rCS (9 mg kg^{-1} per day) or control diluent (sterilized saline containing 10% dimethylsulfoxide) was administered i.p. to the disease-affected mice (N = 8, 6, 9 and 9, respectively) for 10 days from the day before the injection of mAbs (days –3 to 6).

Clinical and histopathological assessment of murine arthritis

The severity of the arthritis was evaluated macroscopically for every paw with a scoring system as follows: 0 = intact, 1 = mild swelling, 2 = severe swelling and 3 = deformed or ankylosed (11), although no deformity or ankylosis was observed in the present study. The sum of the four paws gave a clinical arthritis score, ranging 0–12. The assessments were performed in a blind-test fashion. For histopathological evaluation, the mice were sacrificed on the 19th day after the LPS injection. The right hind paw was resected from each body, fixed with 10% formaldehyde, decalcified in 10% EDTA, embedded in paraffin and stained with hematoxylin and eosin. The histopathological severity was evaluated for the findings of cell infiltration, pannus formation and bone erosion with a scoring system as follows: 0 = no signs, 1 = slight, 2 = moderate and 3 = remarkable. The sum of the three items gave a histopathological arthritis score, ranging 0–9.

Quantification of cytokine mRNA levels at inflamed joints

To analyze the time course of cytokine mRNA expression, the arthritis was induced in 40 BALB/c mice, and 5 mice each were sacrificed 0, 2, 4, 8, 24, 48, 72 or 96 h after the LPS injection. To examine the effects of E-64-d on the cytokine mRNA expression, 32 BALB/c mice affected by the arthritis were treated i.p. with a high dose (9 mg kg^{-1} per day) of E-64-d or control diluent from the day before the injection of mAbs (day –3), until they were sacrificed at the 4th or 48th h after the LPS injection (N = 8; given the same treatment and sacrificed at a time). Then the four paws of each mouse were resected from the body and homogenized altogether in 6 ml of TRIzol reagent (Invitrogen, Carlsbad, CA, USA). Total RNA was purified with the RNeasy Mini Kit (Qiagen, Valencia, CA, USA) and the cDNA was synthesized by random hexamer priming with the TaqMan reverse transcription (RT) reagents (Applied Biosystems, Foster City, CA, USA). The amount of cytokine mRNA was determined with a quantitative real-time RT–PCR system (ABI PRISM 7700 Sequence Detection System, Applied Biosystems). Briefly, the cDNA was amplified with the primers and probes for the targeted cytokine (IL-1α, IL-1β, IL-6 or TNF-α) mRNA and control 18S rRNA, which were available commercially (Applied Biosystems). The data were analyzed by the Sequence Detector software (Applied Biosystems). *Ct* values (cycle numbers to the threshold) for each of the targeted mRNA were normalized by subtracting *Ct* values for 18S rRNA (ΔCt), i.e. the quantities of the targeted mRNA were normalized by the quantities of control 18S rRNA. The normalized mRNA quantities (proportional to $2^{-\Delta Ct}$) were

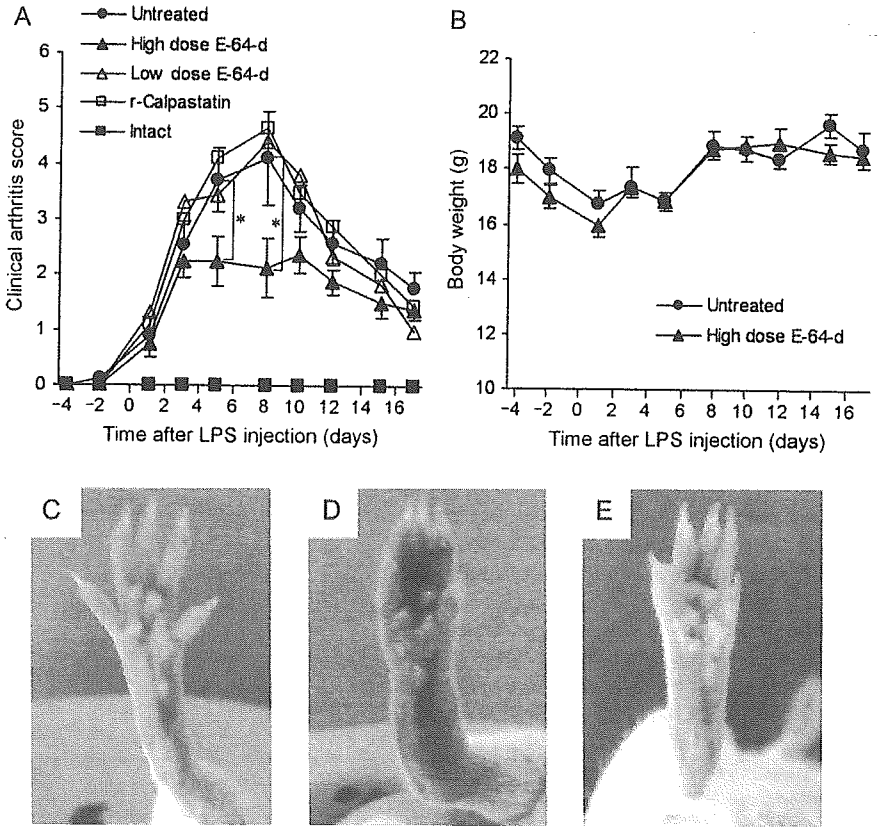

Fig. 1. Effects of calpain inhibitors on mice with anti-type II CL antibody-induced arthritis. Arthritis was induced in 7-week-old BALB/c mice with anti-type II CL mAbs (day −2) and LPS (day 0). To alleviate the arthritis, a high dose (9 mg kg^{-1} per day) or low dose (3 mg kg^{-1} per day) of E-64-d, rCS (9 mg kg^{-1} per day) or control diluent was administered for 10 days (days −3 to 6). (A and B) Time courses of the clinical arthritis scores and body weight of the mice, which were treated or not treated with calpain inhibitors. SEMs are indicated for the untreated group and the high-dose E-64-d group. $*P < 0.05$ between the untreated group and the high-dose E-64-d group. (C–E) Representative macroscopic images of the hind paws photographed on day 8. (C) A non-manipulated mouse. (D) A disease-affected mouse, whose hind paws are swollen severely. (E) A disease-affected mouse that was treated with a high dose of E-64-d, whose hind paws are less affected than in (D).

compared among the experimental groups ($\Delta\cdot\Delta Ct$ method). We fixed the mRNA quantities at the fourth hour after the LPS injection in the control group as 100%, and relative mRNA quantities were calculated.

Cell line and synoviocytes

E11, a fibroblast-like synovial cell line established from knee joint tissues of a RA patient (26), was kindly provided by Y. Tanaka (University of Occupational and Environmental Health, Kitakyushu, Japan). Crude synoviocytes were obtained from joint tissues of a RA patient who fulfilled the American College of Rheumatology criteria, as described elsewhere (9). Briefly, the synovial membrane was cut into small pieces and digested with 0.25% collagenase (type S-1, Nitta Gelatin, Osaka, Japan). E11 cells and the crude synoviocytes were cultured in RPMI 1640 medium containing 10% FCS, 100 IU ml^{-1} penicillin G and 100 μg ml^{-1} streptomycin at 37°C in a 5% CO_2 incubator. The crude synoviocytes were subjected to the assays on the third passage. The following *in vitro* assays were triplicated.

Cytokine production assay

E11 cells (1×10^4 per 200 μl per well) were seeded in a 96-well microplate and incubated for 12 h. After the supernatants were exchanged for new medium, the cells were treated with various concentrations of E-64-d, E-64, rCS or control (2% dimethylsulfoxide) for 24 h in the presence or absence of 10 ng ml^{-1} PMA plus 750 ng ml^{-1} IM. Then, the supernatant cytokines were quantified by ELISA (Cytoscreen ELISA Kit, Biosource, Camarillo, CA, USA). To quantify the intracellular cytokines, E11 cells (1×10^5 ml^{-1} per well) were seeded in a 24-well microplate, incubated for 12 h and treated with each of the calpain inhibitors for 24 h. Then, the supernatants were removed, and the cells were lysed with 500 μl of a solution containing 0.1% Triton X-100, 20 mM HEPES–NaOH (pH 7.9), 300 mM NaCl, 10 mM KCl, 1 mM $MgCl_2$, 20% glycerol, 0.5 mM phenylmethylsulfonylfluoride and 0.5 mM dithiothreitol. After centrifugation at 6000 × *g* for 5 min, the supernatant cytokines were quantified by ELISA.

Cell proliferation assay

A colorimetric cell viability assay was performed with a water-soluble tetrazolium salt-1 (WST-1) solution (Cell Counting Kits, Dojindo Laboratories, Kumamoto, Japan). Briefly, E11 cells (1×10^4 per 200 μl per well) were seeded in a 96-well microplate, incubated for 12 h and treated with each of the calpain inhibitors or 2.5% sodium azide for 20 h. Then, the

WST-1 solution (10 μl per well) was added, and the culture was continued for an additional 4 h. The number of viable cells was estimated by measuring the optical density at 450 nm (corrected by subtracting the optical density at 600 nm) with a microplate reader (model 550, Bio-Rad, Hercules, CA, USA).

Statistical analysis

Cell counts, mRNA levels and cytokine concentrations were compared among the experimental groups by the unpaired Student's *t*-test, whereas clinical and histopathological arthritis scores were compared by the Mann–Whitney *U*-test. *P*-values <0.05 were considered significant.

Results

Efficacy of calpain inhibitors in murine arthritis

To examine the therapeutic effects of calpain inhibitors on arthritis *in vivo*, experimental arthritis was induced with anti-type II CL mAbs and LPS (25) in the BALB/c strain, which is highly susceptible to this system (11, 27). Similar to a previous report (11), signs of arthritis emerged around 48 h after the LPS injection, peaked at around the eightth day (Fig. 1D) and remitted gradually (Fig. 1A). To prevent the development of the disease, a high dose or low dose of E-64-d or rCS was administered. In the macroscopic examination, the high-dose E-64-d group exhibited significantly lower clinical arthritis scores than the untreated group, while the low-dose E-64-d group and the rCS-treated group showed no improvements (Fig. 1A). The paws of the mice treated with a high dose of E-64-d were less affected than those of the untreated mice (Fig. 1D and E). In the microscopic evaluation, the joints of the mice treated with a high dose of E-64-d showed lighter findings than those of the untreated mice, which exhibited typical arthritic findings such as inflammatory cell infiltration, pannus formation and bone erosion (Fig. 2C and D). The histopathological score for cell infiltration and the total histopathological arthritis score in the high-dose E-64-d group were significantly lower than those in the untreated group (Fig. 2A). E-64-d was considered to be safe since there were no significant differences in macroscopic findings or body weight between the high-dose E-64-d group and the untreated group, although both groups of mice lost weight transiently after the LPS injection (Fig. 1B).

Effects of E-64-d on cytokine expression in vivo

We examined the time courses of IL-1α, IL-1β, IL-6 and TNF-α mRNA expression at the inflamed joints of the disease-affected mice by quantitative RT-PCR. The IL-6 and IL-1β mRNA levels showed prominent surges around 4 h after the LPS injection, then dropped and gradually increased again from around the 48th to the 72nd h (Fig. 3A and B, solid lines). When we examined the effects of LPS alone, the second peaks were not observed (Fig. 3A and B, broken lines). Compared with the IL-6 and IL-1β mRNA, the TNF-α and IL-1α mRNA levels showed different patterns, increasing around the fourth hour and remaining elevated for ~24 h, and then gradually decreasing (Fig. 3C and D). Next, we administered E-64-d to the mice and examined its effects on the cytokine mRNA expression. At the fourth hour, none of the cytokine mRNA levels was affected by E-64-d (Fig. 4). At the 48th h, the IL-6 and IL-1β mRNA levels were significantly decreased by E-64-d, compared with those of the untreated mice (Fig. 4A and B).

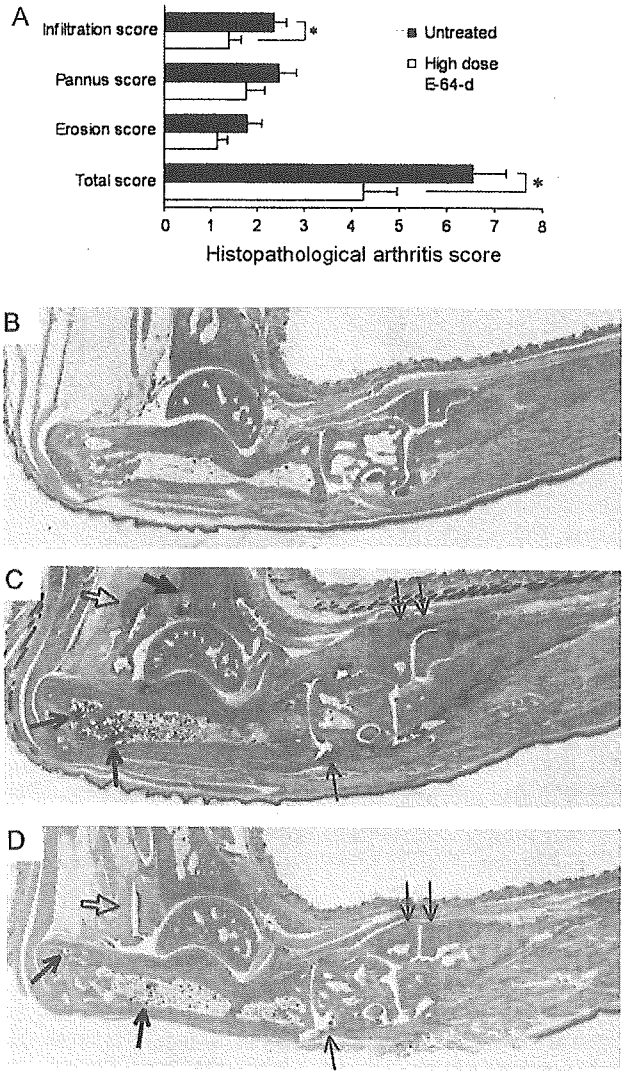

Fig. 2. Effects of calpain inhibitors on histopathological findings of the inflamed joints. The hind paws were sampled on the 19th day after the LPS injection, and hematoxylin- and eosin-stained specimens were prepared. (A) Histopathological arthritis scores are compared between the untreated group and the high-dose (9 mg kg^{-1} per day) E-64-d group. (B–D) Representative microscopic images of the joints. (B) A non-manipulated mouse. (C) A disease-affected mouse, exhibiting typical arthritic findings such as bone erosion (filled arrow), pannus formation (opened arrow), inflammatory cell infiltration (thick arrows) and synovial proliferation (thin arrows). (D) A disease-affected mouse that was treated with a high dose of E-64-d, exhibiting lighter findings than in (C).

Effects of calpain inhibitors on cytokine production in vitro

To examine the effects of the calpain inhibitors *in vitro*, we used a fibroblast-like synovial cell line (E11) established from knee joint tissues of a RA patient (26). After E11 cells were treated with E-64-d, E-64 or rCS, the supernatant IL-6 was quantified by ELISA. We found that E11 cells spontaneously secreted